Synthesis, Characterization, and Theoretical Study of Sulfur-Containing Donor−Acceptor DCNQI Derivatives with Photoinduced Intramolecular Electron Transfer

Nazario Martín,* José L. Segura, and Carlos Seoane*

Departamento de Química Orgánica, Facultad de Química, Universidad Complutense, E-28040 Madrid, Spain

Enrique Ortí, Pedro M. Viruela, and Rafael Viruela

Departamento de Química Física, Universidad de Valencia, E-46100 Burjassot (Valencia), Spain

Armando Albert and Félix H. Cano

Departamento de Cristalografía, Instituto Rocasolano (CSIC), Serrano 116, E-28006 Madrid, Spain

José Vidal-Gancedo, Concepció Rovira, and Jaume Veciana

Institut de Ciència de Materials de Barcelona (CSIC) , Campus U.A.B., E-08193 Bellaterra, Spain

Received December 28, 1995[⊗]

The donor−acceptor compounds *N,N′*-dicyanobenzo[*b*]naphtho[2,3-*e*][1,4]dithiin-6,11-quinonediimine (**9a**) and *N,N′*-dicyanobenzo[*b*]naphtho[2,3-*e*][1,4]oxathiin-6,11-quinonediimine (**10a**) and their methyl-substituted derivatives (**9b** and **10b**−**d**, respectively) have been prepared, and their structural and electronic properties have been characterized by both experimental techniques and quantum-chemical calculations. The ^{1}H-NMR spectra evidence the existence of a *syn*/*anti* isomerism in solution. Both experimental and theoretical data suggest that the preferred configuration of the N−CN groups corresponds to a *syn* isomer for **9** and to an *anti* isomer for **10**. The X-ray analysis performed for **9b** reveals that molecules are not planar and pack in vertical stacks showing an overlap between donor and acceptor moieties of adjacent molecules. In agreement with X-ray data, theoretical calculations predict that both for **9** and **10** the acceptor DCNQI moiety is folded and adopts a butterfly-type structure and the donor moiety is bent along the line passing through the heteroatoms. The energy difference between planar and butterfly structures is calculated to be < 3 kcal/mol at the *ab initio* 6-31G* level. The UV-vis spectra present a broad absorption in the visible which corresponds to a photoinduced intramolecular electron transfer from the high-energy HOMO furnished by the donor moiety to the low-energy LUMO located on the DCNQI fragment. Cyclic voltammetry displays one oxidation peak to the cation and two one-electron reduction waves to the anion and dianion. Theoretical calculations show the planarization of the acceptor/donor moiety induced by reduction/oxidation. The formation of stable radical anions is corroborated by the intense EPR signals recorded for reduced **9**. The assignment of the hyperfine coupling constants of the EPR spectra is consistent with the existence of a preferred *syn* configuration.

Introduction

A great deal of work has been devoted to the synthesis and study of new conducting materials derived from strong donor molecules, mainly tetrathiafulvalene (TTF, **1**)[1] and bis(ethylenedithio)tetrathiafulvalene (BEDT-TTF, **2**)[2] and their derivatives including selenium and tellurium analogues,[3] and/or from strong acceptor molecules, mainly tetracyano-*p*-quinodimethane (TCNQ, **3**)[4] and, more recently, *N,N′*-dicyano-*p*-quinonediimine (DCNQI, **4**) and their derivatives.[5] This effort has led to the preparation of a large variety of charge-transfer salts and intermolecular charge-transfer complexes (CTC) between donor and acceptor molecules exhibiting conducting properties as semiconductors, conductors, and superconductors.[6]

A lower number of examples is known in which both the electron donor and the electron acceptor belong to the same organic molecule.[7] In addition to the conducting properties, single-component donor−acceptor compounds are interesting as potential "molecular electronic devices" showing unidirectional electron flow[8] and as molecular chromophores with nonlinear optical (NLO) properties[9] or solvatochromic effects.[10]

In this context, we have recently reported the synthesis, electrochemistry, and structural properties of a series of novel single-component donor−acceptor organic semiconductors derived from TCNQ (**5**, **6**).[11] The UV-vis spectra of these compounds show the presence of a broad absorption in the visible which was attributed to an intramolecular charge transfer between the donor and acceptor moieties. Their donor−acceptor character was further evidenced by electrochemical measurements which, demonstrated the formation of stable cations and anions. X-ray analysis and theoretical calculations revealed that the molecular structure of compounds **5** and **6** is severely distorted from planarity due, mainly, to the strong steric interactions that take place between the cyano groups and the atoms in *peri* positions.In this paper we describe the synthesis, spectroscopy, electrochemistry, and crystallographic properties of novel sulfur-containing donor−acceptor molecules derived from DCNQI (**9**, **10**). Theo-

[⊗] Abstract published in *Advance ACS Abstracts,* April 1, 1996.

S0022-3263(95)02274-2 CCC: $12.00

Chart 1

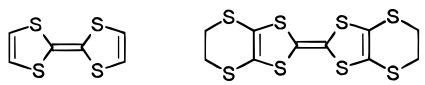

TTF, 1

BEDT-TTF, 2

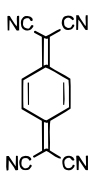

TCNQ, 3

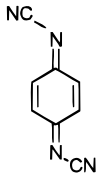

DCNQI, 4

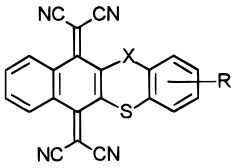

5: X = S
6: X = O

retical calculations are performed to help in the understanding of the molecular and electronic structures and of their evolution upon reduction or oxidation. EPR measurements for the anions of **9** are also reported. The presence of the more flexible cyanoimino group (=NCN) instead of the rigid dicyanomethylene group [=C(CN)$_2$] should, in principle, mitigate the steric hindrance found for the TCNQ derivatives **5** and **6**. The parent DCNQI molecule has an acceptor strength comparable to that of the TCNQ molecule, and its tetrasubstituted derivatives show a molecular structure considerably more planar than the respective TCNQ derivatives.[12]

Results and Discussion

Synthesis. The target molecules **9** and **10** were prepared from benzo[*b*]naphtho[2,3-*e*][1,4]dithiin-6,11-quinones (**7**) and benzo[*b*]naphtho[2,3-*e*][1,4]oxathiin-6,-11-quinones (**8**)[11] by following Hünig's procedure.[5a] The reaction of **7** and **8** with excess of bis(trimethylsilyl)-carbodiimide (BTC) in dichloromethane and in the presence of titanium tetrachloride yields the corresponding DCNQI derivatives as colored, high melting point, microcrystalline solids in very good yields (see Table 1).

(1) See for example: (a) Wudl, F.; Smith, G. M.; Hufnagel, E. J. *J. Chem. Soc., Chem. Commun.* **1970**, 1453. (b) Bryce, M. R. *Aldrichim. Acta* **1985**, *18*, 73. (c) Aharon-Shalom, E.; Becker, J. Y.; Bernstein, J.; Bittner, S.; Shaik, S. *Tetrahedron Lett.* **1985**, 2783. (d) Hsu, S.-Y.; Chiang, L. Y. *Synth. Met.* **1988**, *27*, B651. (e) Chen, W.; Cava, M. P.; Takassi, M. A.; Metzger, R. M. *J. Am. Chem. Soc.* **1988**, *110*, 7903. (f) Rovira, C.; Santaló, N.; Veciana, J. *Tetrahedron Lett.* **1989**, *30*, 7249. (g) Adam, M.; Wolf, P.; Räder, H.-J.; Müllen, K. *J. Chem. Soc., Chem. Commun.* **1990**, 1624. (h) Sallé, M.; Gorgues, A.; Jubault, M.; Gouriou, Y. *Synth. Met.* **1991**, *42*, 2575. (i) Bryce, M. R.; Marshallsay, G. J. *Tetrahedron Lett.* **1991**, 6033. (j) Becker, J. Y.; Bernstein, J.; Bittner, S.; Shahal, L.; Shaik, S. S. *J. Chem. Soc., Chem. Commun.* **1991**, 92. (k) Iyoda, M.; Kuwatani, Y.; Ueno, N.; Oda, M. *J. Chem. Soc., Chem. Commun.* **1992**, 158. (l) Fabre, J.-M.; Garín, J.; Uriel, S. *Tetrahedron* **1992**, *48*, 3983. (m) Bryce, M.; Marshallsay, G. J.; Moore, A.-J. *J. Org. Chem.* **1992**, *57*, 4859. (n) Bryce, M. R.; Coffin, M. A.; Clegg, W. *J. Org. Chem.* **1992**, *57*, 1696. (o) Röhrich, J.; Müllen, K. *J. Org. Chem.* **1992**, *57*, 2374. (p) Sudmale, I. V.; Tormos, G. V.; Khodorkovsky, V. Y.; Edzina, A. S.; Neilands, O. J.; Cava, M. P. *J. Org. Chem.* **1993**, *58*, 1355. (q) Giffard, M.; Frère, P.; Gorgues, A.; Riou, A.; Roncali, J.; Toupec, L. *J. Chem. Soc., Chem. Commun.* **1993**, 944. (r) Tachikawa, T.; Izuoka, A.; Sugawara, T. *J. Chem. Soc., Chem. Commun.* **1993**, 1227. (s) Adam, M.; Fanghänel, E.; Müllen, K.; Shen, Y.-J.; Wegner, R. *Synth. Met.* **1994**, *66*, 275. (t) Kux, U.; Yyoda, M. *Chem. Lett.* **1994**, 2327. (u) Otsubo, T.; Kochi, Y.; Bitoh, A.; Ogura, F. *Chem. Lett.* **1994**, 2047. (v) Aqad, E.; Becker, J. Y.; Bernstein, J.; Ellern, A.; Khodorkovsky, V.; Shapiro, L. *J. Chem. Soc., Chem. Commun.* **1994**, 2775. (x) Wang, C.; Ellern, A.; Khodorkovsky, V.; Becker, J. Y.; Bernstein, J. *J. Chem. Soc., Chem. Commun.* **1994**, 2115. (y) Lahlil, K.; Moradpour, A.; Merienne, C.; Bowlas, Ch. *J. Org. Chem.* **1994**, *59*, 8030. (z) Becher, J.; Lau, J.; Leriche, P., Mork, P.; Svenstrup, N. *J. Chem. Soc., Chem. Commun.* **1994**, 2715. (aa) Batsanov, A. S.; Bryce, M. R.; Cooke, G.; Dhindsa, A. S.; Heaton, J. N.; Howard, J. A. K.; Moore, A. J.; Petty, M. C. *Chem. Mater.* **1994**, *6*, 1419. (bb) Dolbecq, A.; Fourmigué, M.; Batail, P.; Coulon, C. *Chem. Mater.* **1994**, *6*, 1413. (cc) Rovira, C.; Veciana, J.; Santaló, N.; Tarrés, J.; Cirujeda, J.; Molins, E.; Llorca, J.; Espinosa, E. *J. Org. Chem.* **1994**, *59*, 3307. (dd) Jorgensen, T; Hansen, T. K.; Becher, J. *Chem. Soc. Rev.* **1994**, 41. (ee) Yamada, J.; Amano, Y.; Takasaki, S; Nakanishi, R.; Matsumoto, K.; Satoki, S.; Anzai, H. *J. Am. Chem. Soc.* **1995**, *117*, 1149. (ff) Gomper, R.; Hock, J.; Polborn, K., Dormann, E., Winter, H. *Adv. Mater.* **1995**, *7*, 41. (gg) Lorcy, D.; Carlier, R.; Robert, A.; Tallec, A.; Le Maguerès, P.; Ouhab, L. *J. Org. Chem.* **1995**, *60*, 2443. (hh) Benahmed-Gasmi, A.; Fère, P.; Roncali, J.; Elandaloussi, E.; Orduna, J.; Garín, J.; Jubault, M.; Gorgues, A. *Tetrahedron Lett.* **1995**, *36*, 2983. (ii) Neilands, O.; Belyakov, S.; Tilika, V.; Edzina, A. *J. Chem. Soc., Chem. Commun.* **1995**, 325. (jj) Leriche, P.; Gorgues, A.; Jubault, M.; Becher, J.; Orduna, J.; Garín, J. *Tetrahedron Lett.* **1995**, *36*, 1275.

(2) See for example: (a) Kini, A. M.; Beno, M. A.; Williams, J. M. *J. Chem. Soc., Chem. Commun.* **1987**, 335. (b) Moore, A. J.; Bryce, M. R.; Ando, D. J.; Hursthouse, M. B. *J. Chem. Soc., Chem. Commun.* **1991**, 320. (c) Hansen, T. K.; Lakshmikantham, M. V.; Cava, M. P.; Metzger, R. M.; Becher, J. *J. Org. Chem.* **1991**, *56*, 2720. (d) Blanchard, Ph.; Sallé, M.; Duguay, G.; Jubault, M.; Gorgues, A. *Tetrahedron Lett.* **1992**, *33*, 2685. (e) Bryce, M. R.; Coffin, M. A. *J. Org. Chem.* **1992**, *57*, 1696. (f) Frère, P.; Carlier, R.; Boubekeur, K.; Gorges, A.; Roncali, J.; Tallec, A.; Jubault, M.; Batail, P. *J. Chem. Soc., Chem. Commun.* **1994**, 2071. (g) Chou, L.-K.; Quijada, M. A.; Clevenger, M. B.; de Oliveira, G. F., Abboud, K. A.; Tanner, D. B.; Talham, D. R. *Chem. Mater.* **1995**, *7*, 530.

(3) See for example: (a) Wudl, F.; Aharon-Shalom, E. *J. Am. Chem. Soc.* **1982**, *104*, 1154. (b) Jackson, Y. A.; White, C. L.; Lakshmikantham, M. V.; Cava, M. P. *Tetrahedron Lett.* **1987**, 5635. (c) McCullough, R. D.; Kok, G. B.; Lerstrup, K. A.; Cowan, D. O. *J. Am. Chem. Soc.* **1987**, *109*, 4115. (d) Sallé, M.; Gorgues, A.; Fabre, J. M.; Bechgaard, K.; Jubault, M.; Textier, F. *J. Chem. Soc., Chem. Commun.* **1989**, 1520. (e) Kobayashi, K.; Kikuchi, K.; Koide, A.; Ishikawa, Y. Saito, K.; Ikemoto, I. *J. Chem. Soc., Chem. Commun.* **1992**, 1198. (f) Moore, A. J.; Bryce, M. R.; Cooke, G.; Marshallsay, G. J.; Skabara, P. J.; Batsanov, A. S.; Howard, J. A. K.; Daley, S. T. A. *J. Chem. Soc., Perkin Trans. 1* **1993**, 1403.

(4) (a) Wheland, R. C.; Martin, E. L. *J. Org. Chem.* **1975**, *40*, 3101. (b) Yamaguchi, S.; Tatemitsu, H.; Sakata, Y.; Misumi, S. *Chem. Lett.* **1983**, 1229. (c) Aumuller, A.; Hünig, S. *Liebigs Ann. Chem.* **1984**, 618; Ong, B. S.; Keoshkerian, B. *J. Org. Chem.* **1984**, *49*, 5002. (d) Kini, A. M.; Cowan, D. O.; Gerson, F.; Mockel, R. *J. Am. Chem. Soc.* **1985**, *107*, 556. (e) Martín, N.; Hanack, M. *J. Chem. Soc., Chem. Commun.* **1988**, 1522. (f) Martín, N.; Behnish, R.; Hanack, M. *J. Org. Chem.* **1989**, *54*, 2563. (g) Cruz, P.; Martín, N.; Miguel, F.; Seoane, C.; Albert, A.; Cano, F. H.; González, A.; Pingarrón, J. M. *J. Org. Chem.* **1992**, *57*, 6192. (h) Tsubata, Y.; Suzuki, T.; Miyasahi, T.; Yamashita, Y. *J. Org. Chem.* **1992**, *57*, 6749. (i) Iwatsuki, S.; Kubo, M.; Iwase, H. *Chem. Lett.* **1993**, 517. (j) Yanagimoto, T.; Takimiya, K.; Otsubo, T.; Ogura, F. *J. Chem. Soc., Chem. Commun.* **1993**, 519. (k) Fujii, M.; Aso, Y.; Otsubo, T.; Ogura, F. *Synth. Met.* **1993**, *55*−57, 2136. (l) Martín, N.; Segura, J. L.; Seoane, C.; Torío, C.; González, A.; Pingarrón, J. M. *Synth. Met.* **1994**, *64*, 83. (m) Rule, N. G.; Detty, M. R.; Kaeding, J. E.; Sinicropi, J. A. *J. Org. Chem.* **1995**, *60*, 1665. (n) Bryce, M. R.; Murphy, L. C. *Nature* **1984**, *309*, 119.

(5) (a) Aumüller, A.; Hünig, S. *Angew. Chem., Int. Ed. Engl.* **1984**, *96*, 437. (b) Aumüller, A.; Hünig, S. *Liebigs Ann. Chem.* **1986**, 142. (c) Hünig, S. *Pure Appl. Chem.* **1990**, *62*, 395. (d) Günther, E.; Hünig, S.; Peters, K.; Rieder, H.; Schnering, H. G.; Schütz, J.-U.; Söderholm, S.; Werner, H.-P.; Wolf, H. C. *Angew. Chem., Int. Ed. Engl.* **1990**, *29*, 204. (e) Hünig, S.; Erk, P. *Adv. Mater.* **1991**, *5*, 225. (f) Martín, N.; Navarro, J. A.; Seoane, C.; Albert, A, Cano, F. H.; Becker, J. Y.; Khodorkovsky, V.; Harlev, E.; Hanack, M. *J. Org. Chem.* **1992**, *57*, 5726. (g) Hünig, S.; Sinzger, K.; Jopp, M.; Bauer, D.; Bietsch, W.; Ulrich, J.; Wolf, H. C. *Angew. Chem., Int. Ed. Engl.* **1992**, *31*, 859. (h) Barranco, E.; Martín, N.; Segura, J. L.; Seoane, C.; Cruz, P.; Langa, F.; González, A.; Pingarrón, J. M. *Tetrahedron* **1993**, *49*, 4881. (i) Kobayashi, H. *J. Am. Chem. Soc.* **1993**, *115*, 7870. (j) González, M.; de Miguel, P.; Martín, N.; Segura, J. L.; Seoane, C.; Ortí, E.; Viruela, R.; Viruela, P. M. *Adv. Mater.* **1994**, *6*, 765. (k) Martín, N.; Seoane, C.; Garín, J.; Orduna, J. *Rapid Commun. Mass Spectr.* **1995**, *9*, 71 .

(6) For a review see: (a) Bryce, M. R. *Chem. Soc. Rev.* **1991**, *20*, 355. (b) Cowan, D. O.; Wlygul, F. M. *Chem. Eng. News* **1986**, *64*, 28. (c) Wudl, F. *Acc. Chem. Res.* **1984**, *17*, 227. (d) Torrance, J. B. *Acc. Chem. Res.* **1979**, 12, 79. See also: (e) *Organic Superconductors*; Ishiguro, T., Yamaji, K., Eds., Springer-Verlag: Berlin, 1990. (f) *Organic Superconductors (including Fullerenes)*; Williams, J. M., Ferraro, J. R., Thorn R. J., Carlson, K. D., Geiser, U., Wang, H. H., Kini, A. M., Whangbo, M.-H.; Prentice Hall: New Jersey, 1992.

Table 1. Novel Donor−Acceptor Compounds Prepared

compound	R_1	R_2	R_3	yield (%)	mp, °C	λ_{max} (log ϵ)[a]	ν_{CN}[b]
7a[c]	H	H	H	73	288−290	542 (2.92)	−
8a[c]	H	H	H	82	256−258	548 (2.94)	−
9a	H	H	H	87	>300	628 (3.94)	2180
9b	H	Me	H	92	>300	644 (3.74)	2180
10a	H	H	H	83	>300	669 (3.05)	2170
10b	H	Me	H	93	>300	692 (3.06)	2180
10c	H	H	Me	89	>300	688 (3.09)	2180
10d	Me	H	Me	77	>300	717 (3.18)	2180

[a] In nm. Solvent: $CHCl_3$. [b] In KBr pellets (cm^{-1}). [c] For comparison purposes.[11]

Chart 2

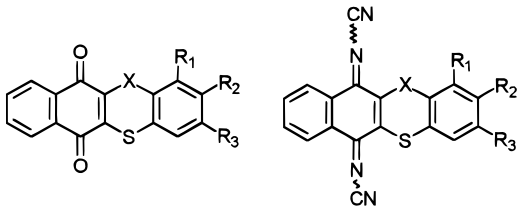

7: X = S
8: X = O

9: X = S
10: X = O

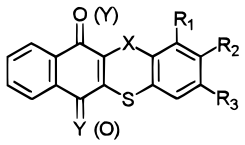

Y: N-CN

11: X = S

12: X = O

The cyanoimino derivatives **11** and **12** resulting from the monocondensation reaction were prepared by using a lower amount of BTC and $TiCl_4$ and shorter reaction times. They were obtained in moderate yields as a mixture of two constitutional isomers as shown by high resolution ^{1}H-NMR spectra (see Experimental Section).

Chart 3

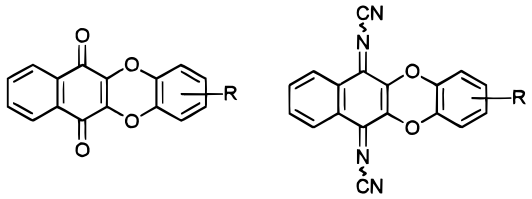

13 14

Chart 4

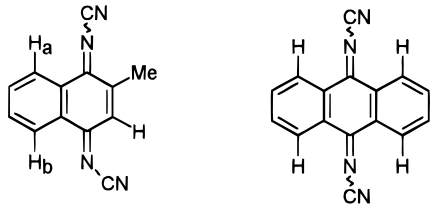

15 16

Attempts to separate them by using chromatographic procedures were unsuccessful due to their instability on silica gel.

The synthesis of the *N*,*N*′-dicyano-*p*-quinonediimine derivatives **14** from the corresponding benzo[*b*]naphtho-[2,3-*e*][1,4]-dioxin-6,11-quinones (**13**) was previously described as intended donor−acceptor systems.[13] No UV-vis data were reported.

NMR Spectroscopy. The high resolution ^{1}H-NMR spectra of compounds **9** and **10** evidence that these DCNQI derivatives exist as a mixture of isomers in which the NCN groups adopt different orientations with respect to the substituents of the DCNQI ring. The existence of a *syn* ⇌ *anti* isomerization equilibrium for DCNQI derivatives was first established by Hünig *et al*.[5b] These authors suggested the presence of different favored isomers depending upon the number of substituents attached to the DCNQI ring. As depicted in the central chart inserted in Figure 1, a maximum of three isomers can be expected for compounds **9**. Isomers A and C correspond to *syn* orientations in which both NCN groups point to adjacent hydrogens in *peri* positions or to sulfur atoms, respectively. Isomer B has the NCN groups *anti*, pointing to opposite directions.

The ^{1}H-NMR spectrum recorded for **9a** at room temperature (Figure 1) shows a very broad signal centered at $\delta = 8.94$ for the *peri* hydrogens H_a and H_b which is hardly detected. The broadening of this signal, which exhibits no line structure, is indicative of a fast isomerization between the *syn* and *anti* configurations at room temperature. It is interesting to compare this spectrum with the ^{1}H-NMR data reported for the closely related *N*,*N*′-dicyano-2-methyl-1,4-naphthoquinonediimine (**15**) and *N*,*N*′-dicyano-9,10-anthraquinonediimine (**16**).[5b]

For **15**, H_a appears as a broad signal centered at $\delta = 9.16$ and H_b as a doublet at $\delta = 8.42$. The latter appears as a doublet because the adjacent NCN group has a preferred orientation, being in *anti* with respect to H_b. By contrast, the upper NCN group is not configuration-

(7) (a) Aviram, A.; Rattner, M. A. *Chem. Phys. Lett.* **1974**, *29*, 277. (b) Taube, H. *Pure Appl. Chem.* **1975**, *44*, 25. (c) Becker, J. Y.; Bernstein, J.; Bittner, S.; Levi, N.; Shaik, S. S. *J. Am. Chem. Soc.* **1983**, *105*, 4468. (d) Becker, J. Y.; Bernstein, J.; Bittner, S.; Levi, N.; Shaik, S. S.; Zer-Zion, N. *J. Org. Chem.* **1988**, *53*, 1689. (e) Metzger, R. M.; Panetta, C. A. *New. J. Chem.* **1991**, *15*, 209; Panetta, C. A.; Heimer, N. E.; Hussey, C. L.; Metzger, R. M. *Synlett* **1991**, 301. (f) Le Paillard, M. P.; Robert, A.; Garrigon-Lagrange, C.; Delhaes, P.; Le Magnerès, P.; Onahab, L.; Toupet, L. *Synth. Met.* **1993**, 58, 223. (g) Tada, H.; Takenchi, Y.; Amatatsu, Y.; Furnichi, K.; Kato, M.; Matsumoto, S.; Hashimoto, M. *J. Chem. Soc., Perkin Trans. 2* **1993**, 1305. (h) Martín, N.; Segura, J. L.; Seoane, C.; Albert, A.; Cano, F. H. *J. Chem. Soc., Perkin Trans. 1* **1993**, 2363. (i) Staab, H. A.; Feurer, A.; Hauck, R. *Angew. Chem., Int. Ed. Engl.* **1994**, *33*, 2428. (j) Morley, J. O. *J. Phys. Chem.* **1994**, *98*, 13177. (k) Williams, R. M.; Zwier, J. M.; Verhoven, J. W. *J. Am. Chem. Soc.* **1995**, *117*, 4093. (l) Lawson, J. M., Craig, D. C., Oliver, A. M.; Paddon-Row, M. N. *Tetrahedron* **1995**, *51*, 3841.

(8) *Molecular Electronic-Science and Technology*; Aviram, A., Ed.; Engineering Foundation: New York, 1989. See also ref 7.

(9) (a) Boyd, R. W. *Nonlinear Optics*; Academic Press: New York, 1992. (b) Prasad, P. N.; Williams, D. J. *Introduction to Nonlinear Optical Effects in Molecules and Polymers;* Wiley: New York, 1991. (c) Shen, Y. R. *The Principles of Nonlinear Optics*; Wiley: New York, 1984. See also: (d) Di Bella, S.; Fragalá, I. L.; Rattner, M. A.; Marks, T. J. *J. Am. Chem. Soc.* **1993**, *115*, 682. (e) Joshi, M. V.; Cava, M. P.; Lakshikantham, M. V.; Metzger, R. M.; Abdeldayem, H.; Henry, M.; Venkateswarly, P. *Synth. Met.* **1993**, *57*, 3974.

(10) (a) Effenberger, F.; Würthner, F.; Steybe, F. *J. Org. Chem.* **1995**, *60*, 2082. (b) Reichardt, C. *Solvents and Solvent Effects in Organic Chemistry;* 2nd ed.; VCH: Weinheim, 1988.

(11) Bando, P.; Martín, N.; Segura, J. L.; Seoane, C.; Ortí, E.; Viruela, P. M.; Viruela, R.; Albert, A.; Cano, F. H. *J. Org. Chem.* **1994,** *59*, 4618.

(12) (a) Schubert, U.; Hünig, S.; Aumüller, A. *Liebigs Ann. Chem.* **1985**, 1216. (b) Cruz, P.; Martín, N.; Miguel, F.; Seoane, C.; Albert, A.; Cano, F. H.; Leverenz, A.; Hanack, M. *Synth. Met.* **1992**, *48*, 59.

(13) Czekanski, T.; Hanack, M.; Becker, J. Y.; Bernstein, J.; Bittner, S.; Kaufman-Orenstein, L.; Peleg, D. *J. Org. Chem.* **1991**, *56*, 1569.

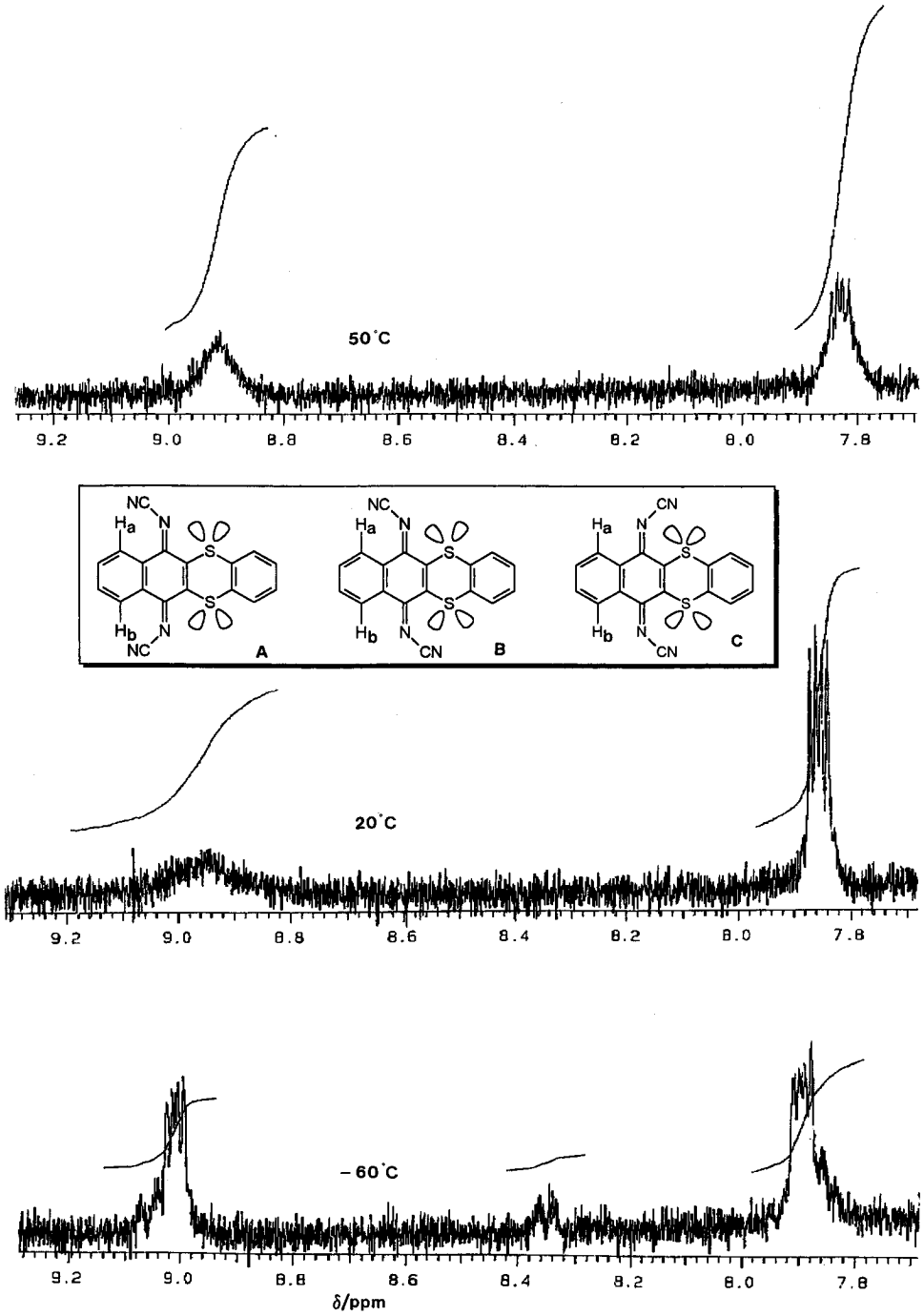

Figure 1. Temperature-dependent ^{1}H-NMR spectra of compound **9a** in $CDCl_3$ at 50 °C (top), 20 °C (center), and −60 °C (bottom).

ally stable and undergoes a rapid *syn*/*anti* isomerization. The shifting of H_a to higher values of δ is due to the deshielding effect expected in the region alongside the cyano group. For **16**, the different orientations of the NCN groups are energetically equivalent, and the four *peri* hydrogens appear as a unique broad signal at δ = 8.70. This value is intermediate between those of H_a (9.16) and H_b (8.42) in **15** and is lower than that of H_a and H_b (8.93) in **9a**, thus indicating that H_a in **15** and H_a and H_b in **9a** are more deshielded than the *peri* hydrogens in **16**. This result suggests that for compounds **9** the most stable orientation of the NCN groups is *anti* with respect to sulfur atoms and isomer A would be the most populated in solution.

In order to achieve a more detailed understanding of the *syn*/*anti* isomerism, the temperature-dependent ^{1}H-NMR spectra of compound **9a** were recorded in $CDCl_3$ from −60 to +50 °C and in deuterated toluene from −70 to +100 °C . Although **9a** resulted in more solubility in toluene, the solvent signals in the aromatic region prevent an accurate analysis of the different isomers. The spectra in $CDCl_3$ are presented in Figure 1 for three different temperatures. A sharpening of the broad signal of the *peri* hydrogens, which now is centered at δ = 8.91, is observed when the temperature is increased to +50 °C. By monitoring the decrease of temperature, the presence of a multiplet centered at δ = 9.00 and two multiplets at δ = 9.06 and 8.35 in an approximate 5:1:1 ratio is detected. The more intense multiplet at δ = 9.00 is assigned to isomer A for which both *peri* hydrogens are equivalent and are deshielded by the NCN groups. The two multiplets at δ = 9.06 and 8.35 integrate to

Chart 5

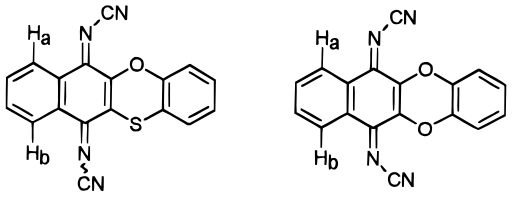

10 14

approximately the same area and are respectively attributed to H_a and H_b of isomer B. Isomer C is not apparently detected due, probably, to its lower stability. This assignment agrees with the suggestion that isomer A is the most stable.

The energy barrier for the *syn*/*anti* isomerization of the NCN groups can be roughly estimated from the coalescence temperature in the ^{1}H-NMR spectra. The coalescence takes place at 283 K for **9a**, and a value of 13.1 kcal/mol is calculated for the free activation energy, $\Delta G_{283}^{\ddagger}$. This value is similar to that obtained for **16** (13.4 kcal/mol) and other substituted DCNQIs.[5b]

The ^{1}H-NMR spectra recorded for compounds **10** at room temperature suggest a different configurational behavior when compared to **9**. The spectrum of **10a** presents a doublet at $\delta = 8.38$ and a broad signal at $\delta = 9.15$. The doublet is assigned to the *peri* hydrogen H_a lying on the same side of the molecule as the oxygen atom. The less voluminous oxygen atom allows the adjacent NCN group to be configurationally stable adopting an *anti* orientation with respect to H_a. The broad singlet at $\delta = 9.15$ is again due to the fast isomerization of the NCN group adjacent to the sulfur atom and is assigned to H_b. These assignments can be ascertained by comparison with the ^{1}H-NMR data previously reported for compound **14** for which the *peri* hydrogens appear at $\delta = 8.33$.[13] Compounds **10** and **14** are therefore better represented by the structures displayed in Chart 5.

The assignments of the NMR signals of the *peri* hydrogens H_a and H_b for compounds **9** and **10** are discussed below on the basis of molecular orbital calculations performed for different isomers.

UV-Vis Spectroscopy. The UV-vis spectra of the DCNQI-derivatives **9** and **10** and of their precursor quinones **7** and **8** reveal, in addition to the expected bands in the UV region, the presence of a very broad, low-energy absorption band in the visible region which undergoes a bathochromic shift when methyl groups are attached to the benzodithiin or benzooxathiin moieties (Table 1). The shift to the red suggests an intramolecular charge transfer from these moieties, whose donor character is enhanced by methyl groups, to the acceptor fragment of the molecule. UV-vis spectra carried out in different dilution conditions confirm the intramolecular nature of this charge-transfer band.

As summarized in Table 1, the value of λ_{max} shifts to higher wavelengths in passing from compounds **9** to **10**. This finding is accounted for by the better donor ability of the benzo[1,4]oxathiin fragment **10** compared to the benzo[1,4]dithiin moiety **9**. For the starting quinones **7** and **8,** the charge-transfer band appears at shorter wavelengths due to the poorer acceptor ability of the carbonyl groups in the quinone ring.

Electrochemistry. The redox potentials of the DCNQI derivatives **9** and **10** were measured in dichloromethane at room temperature by cyclic voltammetry (CV) and are summarized in Table 2. As illustrated in Figure 2 for **9a**, these compounds show an oxidation wave due to the oxidation of the dithiin **9** or oxathiin **10** rings to form the respective cation-radicals, and two one-electron reversible reduction waves to the corresponding anion-radicals and dianions. The half-wave oxidation potentials measured for **9** and **10** are similar to those previously reported for their respective TCNQ analogues **5** and **6**.[11] The existence of two one-electron reduction waves, however, contrasts with the unique two-electron reduction wave observed for **5** and **6**. This different electrochemical behavior was already reported for benzoannulated TCNQs and DCNQIs and was attributed to the higher steric strain present in TCNQ derivatives which largely destabilizes the anion-radical.[14]

The CV data obtained for the first reduction potential reveal that the acceptor moiety in compounds **9** and **10** is a slightly poorer electron acceptor than in the parent DCNQI. By contrast, the values of the second reduction potential of **9** and **10** are similar to that of DCNQI. These trends will be discussed below in terms of the molecular structure optimized for neutral and reduced compounds.

The thermodynamic stability of the anion-radicals is determined by estimating the equilibrium constant K for the coproportionation reaction $A + A^{2-} = 2A^{\bullet -}$. The values of log K (Table 2) are calculated from the difference between the two first reduction potentials ΔE^{red}.[15] Compounds **9** and **10** have similar values of log K, but significantly smaller than that of the parent DCNQI due to the smaller values of ΔE. The values of log K for the

Table 2. Cyclic Voltammetry Data of Donor−Acceptor Compounds (V *vs* SCE)[a]

compound	$E_{1/2}^{ox}$	$E_{1/2}^{1,red}$	$E_{1/2}^{2,red}$	ΔE^{red}	log K[b]
7a[c,d]	1.41	−0.53	−1.09	0.56	9.49
8a[c,d]	1.52	−0.59	−1.09	0.50	8.47
9a	1.51	0.05	−0.36	0.41	7.01
9b	1.43	0.05	−0.34	0.39	6.61
10a	1.64	0.03	−0.42	0.45	7.63
10b	1.54	0.03	−0.43	0.46	7.79
10c	1.56	0.02	−0.44	0.46	7.79
10d	1.51	0.00	−0.42	0.42	7.12
DCNQI[c]	–	0.21	−0.41	0.62	10.50

[a] Electrolyte $Bu_4N^+ClO_4^-$; solvent CH_2Cl_2; scan rate 50 mV s^{-1}. [b] log $K = \Delta E/0.059$; $\Delta E = E_{1/2}^{1,red} - E_{1/2}^{2,red}$. [c] Measured in the same experimental conditions. [d] Data from ref 11.

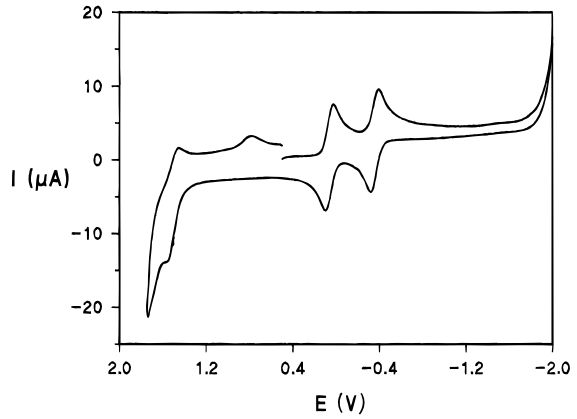

Figure 2. Cyclic voltammogram of compound **9a**. Scan rate: 100 mV s^{-1}.

(14) Aumüller, A.; Hünig, S. *Liebigs Ann. Chem.* **1986**, 165.
(15) Jensen, B. S.; Parker, V. D. *J. Am. Chem. Soc.* **1975**, *97*, 5211.

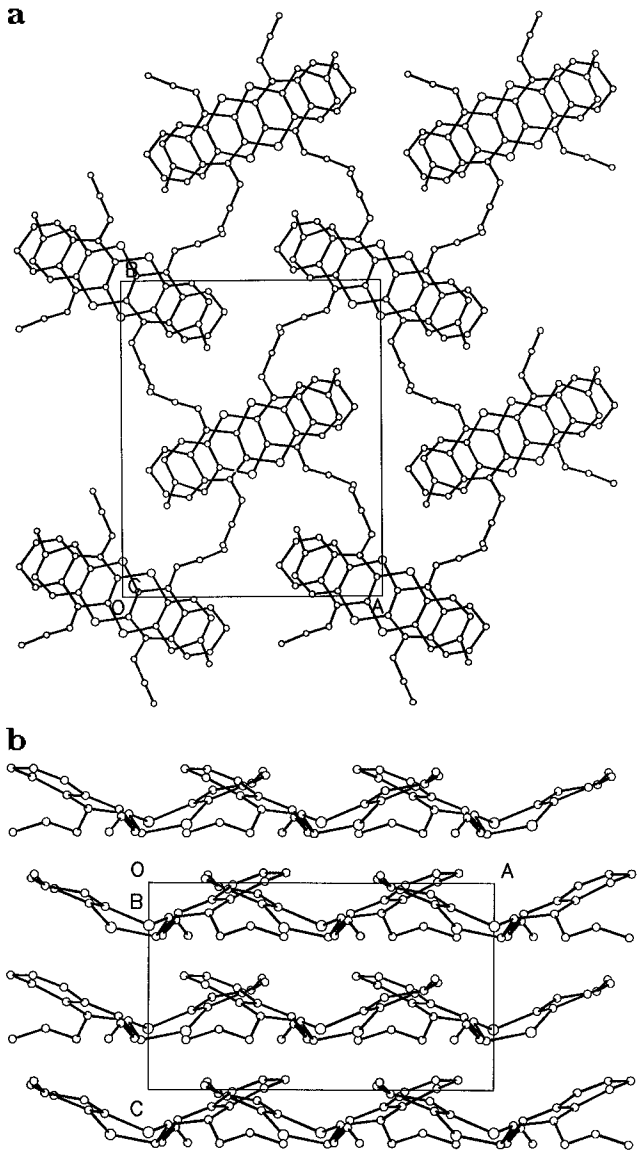

Figure 3. (a) The crystal packing of compound **9b**, as projected along the *b* axis. (b) The crystal packing of compound **9b** showing the aromatic interactions along the *c* axis.

starting quinones **7** and **8** indicate a higher thermodynamic stability of their anion-radicals.

Structural Study. In order to investigate the molecular structure of these donor−acceptor DCNQI derivatives **9**, **10** as well as the intermolecular interactions, the X-ray structural analysis of compound **9b** was carried out.[47] The quality of the crystals, obtained by slow crystallization from acetonitrile, was so poor that for the best one, chosen after many trials, the amount of observed reflections was about one-third of the total data recorded. No highly accurate analysis could therefore be expected, although the overall features and, particularly the packing, are correct (see Experimental Section).

Figure 3 displays two different projections of the crystal packing within a unit cell. The molecules of **9b** are ordered in stacks along the *c* axis, showing an overlap between donor and acceptor moieties of adjacent molecules.[16,17] Both the DCNQI moiety and the dithiin ring are distorted from planarity while the outer benzene rings remain planar as shown in Figure 3.

(16) Desiraju, G. R. *Crystal Engineering*; Elsevier: Amsterdam, 1989.

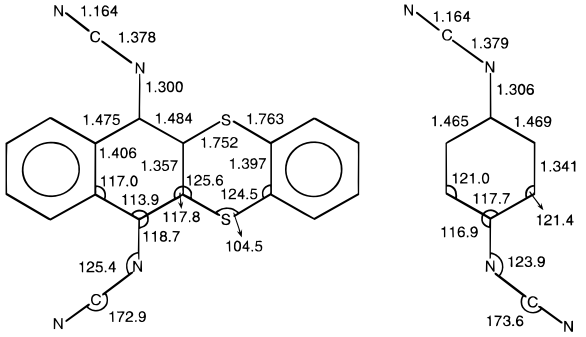

Figure 4. PM3-optimized bond lengths and bond angles for **9a** (C_s symmetry, left) and DCNQI (C_{2h} symmetry, right). Bonds are in angstroms and angles in degrees. The outer benzene rings of **9a** have bond lengths of 1.40 ± 0.01 Å and internal bond angles of 120 ± 1°.

In agreement with the donor−acceptor face-to-face stacking, i.e. a mixed stack mode, the electrical conductivity measured for compressed powder pellets of **9b** by a two-probe technique was lower than 10^{-6} S cm^{-1} at room temperature.

Theoretical Calculations. To gain a deeper understanding of the experimental observations reported above, the molecular and electronic structures of compounds **9a** and **10a** on both neutral and oxidized/reduced states were investigated by performing quantum-chemical calculations at the Hartree−Fock SCF level of approximation. The molecular structure was studied by using both the semiempirical PM3 method and *ab initio* 3-21G and 6-31G* calculations. The electronic structure was investigated by using the nonempirical valence effective Hamiltonian (VEH) pseudopotential technique.

Neutral Compounds: Molecular Structure. Figure 4 displays the PM3 bond lengths and bond angles calculated for **9a** assuming that the perpendicular plane bisecting the molecule along the long molecular axis is a symmetry plane (C_s symmetry). The geometric parameters obtained for DCNQI (C_{2h} symmetry) using the same methodology are included in Figure 4 for the sake of comparison.

Three main results concerning the four-ring backbone of **9a** are inferred from Figure 4: (i) The outer benzene rings preserve their aromatic character, all the C−C bonds having a length of 1.40 ± 0.01 Å and the internal bond angles being of 120 ± 1°. (ii) The DCNQI ring retains its quinoid character. All the C−C bonds forming this ring are slightly lengthened with respect to the parent DCNQI. (iii) The two heteroatom bridges completing the dithiin ring show bond lengths of 1.75−1.76 Å, which are significantly longer than those reported for π-conjugated heterocycles like thiophene where the S−C bonds are of 1.714 Å.[18] This suggests that the acceptor benzo-DCNQI moiety is poorly conjugated with the benzene ring through the heteroatom bridges. All these trends also stand for **10a**, for which no symmetry restriction was imposed during the optimization process.

There are two additional points concerning the molecular structure of compounds **9** and **10** that should be addressed: the planarity of the molecule and the orientation of the NCN groups. Figure 5 presents a series of

(17) Albert, A.; Cano, F. H., CONTACTOS. Computer Program to Study Interactions Between Aromatic Rings. Instituto Rocasolano, C. S. I. C. Serrano, 119. 28006 Madrid. Spain. To be published.

(18) Bak, B.; Christensen, D.; Hansen-Nygaard, L.; Rastrup-Andersen, J. *J. Mol. Spectrosc.* **1961**, *7*, 58.

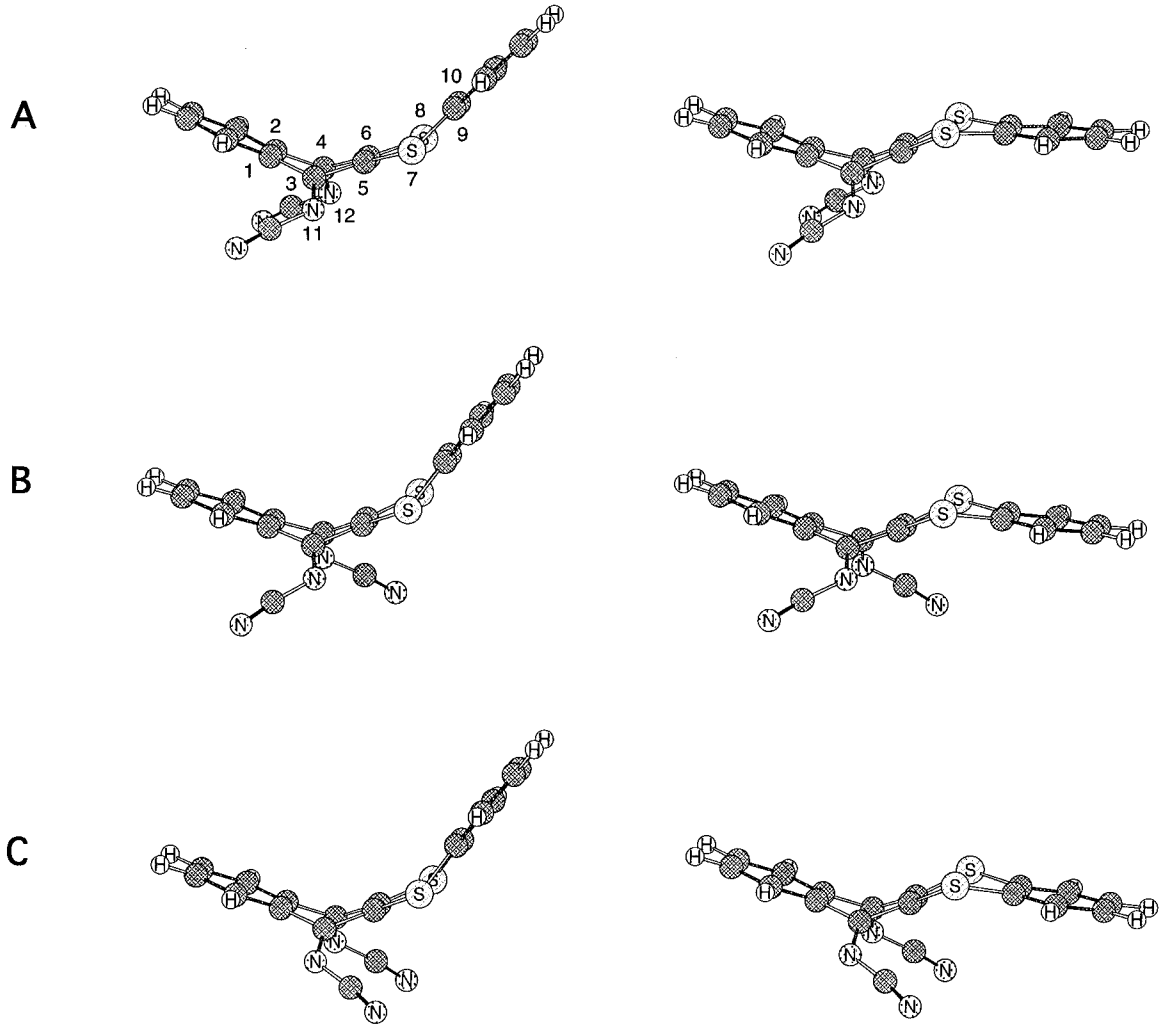

Figure 5. PM3-optimized isomers calculated for **9a**. Isomers A−C result from the relative orientation of the NCN groups and correspond to those depicted in Figure 1. Two dispositions, up (left) and down (right), of the benzodithiine moiety are possible for each isomer.

PM3-equilibrium geometries calculated for **9a**. Structures A−C result from the different orientation of the NCN groups and correspond to the three isomers depicted in Figure 1. For each of these isomers the benzodithiin moiety is found pointing up or down. Similar structures can be drawn for **10a**.

We first focus on the deviations from planarity of the molecular geometry. To avoid the steric interactions between the cyano groups and the atoms in *peri* positions, the DCNQI ring adopts a boat conformation giving rise to a butterfly-type structure similar to that previously obtained for the TCNQ derivatives **5** and **6**.[11] This type of structure was first reported for 11,11,12,12-tetracyano-9,10-anthraquinodimethane (TCAQ) from X-ray crystallographic data.[12a] The analogous DCNQI derivative **16** with 2,3-dimethyl substitution was by contrast predicted to be nearly planar.[12a] The dithiin ring is also bent along the line passing through the sulfur bridges. This bending has been experimentally observed for many thianthrene derivatives[19] and was also found for **5**.[11] The deviations from planarity calculated for **9a** are similar to those observed from X-ray analysis (Figure 3) and do not affect the planarity of the outer benzene rings. Similar foldings are found for compound **10a**.

Table 3. Theoretical Values Calculated for the Dihedral Angles (deg) Defining the Molecular Distortions from Planarity of the Most Stable Conformations of 9a and 10a and of *syn*-16[a]

compound	method	α	β	γ
9a	PM3	141.5	149.9	34.1
10a	PM3	145.5	165.4	29.7
16	PM3	145.7		29.8
	3-21G	167.5		9.8
	6-31G*	153.5		21.9

[a] For compound **10a**, angles α, β, and γ are calculated as the average of the following dihedral angles: α, C1−C3−C4−C6 and C2−C4−C3−C5; β, C5−S7−O8−C10 and C6−O8−S7−C9; γ, C11−C5−C1−C2, C11−C1−C5−C6, C12−C6−C2−C1, and C12−C2−C6−C5. Equivalent definitions are used for the more symmetric **9a** and **16**. See Figure 5 for atom numbering.

Table 3 collects the theoretical values calculated for the dihedral angles describing the deviations from planarity of **9a** and **10a**, together with those obtained for **16**. The folding of the acceptor DCNQI moiety is defined in terms of angles α and γ. α corresponds to the angle formed by the "wings of the butterfly", and γ gives the tilting of the NCN groups with respect to the C1−C2−C5−C6 plane (see Figure 5 for atom numbering). Angle β defines the bending of the dithiin ring.

(19) (a) Lynton, H.; Cox, E. G. *J. Chem. Soc.* **1956**, 4886. (b) Gallaher, K. L.; Bauer, S. H. *J. Chem. Soc., Faraday Trans. 2* **1975**, 1173. (c) Larson, S. B.; Simonsen, S. H. *Acta Cryst. C.* **1984**, *40*, 103. (d) Bock, H.; Rauschenbach, C. N.; Näther, C.; Havlas, Z.; Gavezzotti, A.; Filippini, G. *Angew. Chem., Int. Ed. Engl.* **1995**, *34*, 76.

Table 4. Relative Energies (kcal/mol) Calculated for Different Isomers of 9a and 10a

compound	isomer[a,b]	PM3	6-31G*//PM3
9a	A (up)	0.06	0.00
	(down)	0.00	1.02
	B (up)	0.89	2.75
	(down)	0.19	1.55
	C (up)	1.99	5.28
	(down)	0.77	2.62
10a	A (down)	0.32	2.26
	B (down)	0.00	0.00
	B′ (down)	0.55	4.17
	C (down)	0.56	2.13

[a] Isomers A, B, and C, respectively, correspond to *syn* (NCN groups pointing to the hydrogens in *peri*), *anti*, and *syn* (NCN groups pointing to the heteroatom bridges) orientations of the NCN groups (see Figures 1 and 5). For **10a**, B and B′ correspond to the *anti* isomers in which the NCN group pointing to the heteroatom is that adjacent to the oxygen atom and to the sulfur atom, respectively. [b] Up and down indicate the orientation (β > 180° or β < 180°, respectively) of the lateral benzodithiin (**9a**) or benzooxathiin (**10a**) moieties. For **10a**, isomers with β > 180° (up) were not located as minima at the PM3 level.

The values predicted by the PM3 method for angles α and γ are 141.5° and 34.1° for **9a** and 145.5° and 29.7° for **10a**, respectively. They indicate an important folding of the DCNQI ring similar to that found for the TCNQ ring in **5** (α = 135.2°, γ = 39.9°) and **6** (α = 137.6°, γ = 36.9°).[11] This result agrees with the X-ray structure shown in Figure 3 for **9b**, but contrasts with the nearly planar structure reported for the 2,3-dimethyl derivative of **16**.[12a]

To get a deeper insight on the reliability of the PM3 results, we have fully optimized the molecular geometry of *syn*-**16** with planar and butterfly-type structures at the PM3 level and at the *ab initio* level using the 3-21G and 6-31G* basis sets. At the PM3 level, the butterfly structure (α = 145.7°, γ = 29.8°) is predicted to be 6.24 kcal/mol more stable than the fully planar structure. At the *ab initio* 3-21G level, this energy difference decreases to only 0.07 kcal/mol, and the geometry is only slightly distorted from planarity (α = 167.5°, γ = 9.8°). At the more accurate 6-31G* level, the energy difference increases to 2.75 kcal/mol, and a more distorted geometry (α = 153.5°, γ = 21.9°) is obtained. These energies are much smaller than those obtained for the more hindered TCAQ molecule (28.83 kcal/mol at the PM3 level, 33.45 kcal/mol at the 6-31G* level).[20] Two main conclusions can be therefore inferred from these results: (i) The energy difference between planar and butterfly structures in **16** is small enough to establish that packing interactions will be the driving force which determine the geometry adopted by the DCNQI moiety in the solid in order to achieve the most compact crystal packing. This finding explains the fact that the DCNQI moiety in **9b** is folded to attain the most effective overlap with the donor benzodithiin fragments of the adjacent molecules (see Figure 3), while for the 2,3-dimethyl derivative of **16** is almost planar.[12a] (ii) The PM3 method correctly predicts the folding of the DCNQI moiety even though it overestimates the values of α and γ compared to *ab initio* 6-31G* calculations.

We now turn to discuss the relative stability of the different isomers depicted in Figure 5. Table 4 summarizes the relative energies calculated at the semiempirical PM3 level and at the *ab initio* 6-31G* level using the PM3-optimized geometries (6-31G*//PM3). At both the semiempirical and the *ab initio* levels, the most stable conformation of compound **9a** corresponds to isomer A, where the two NCN groups are in *syn* and point to the adjacent *peri* hydrogens, and the most energetic to isomer C, where both NCN groups point to the sulfur atoms. The steric interactions of the cyano groups with the sulfur atoms are therefore calculated to be more important than the interactions with the *peri* hydrogens. For isomer A, the two possible orientations, up (β > 180°) and down (β < 180°), of the lateral benzodithiin unit are almost isoenergetic at the PM3 level. At the 6-31G*//PM3, the pointing-up structure is more stable by 1.02 kcal/mol in accord with the X-ray structure (see Figure 3). For isomers B and C, the structure with β < 180° is always predicted as the more stable since, in this way, the lone pairs of the sulfur atoms point up and their interaction with the NCN groups is avoided. The energy difference between isomers A and C is therefore of only 0.77 kcal/mol at the PM3 level and increases to 2.62 kcal/mol at the 6-31G*//PM3 level. At this level, the *anti* isomer B has an intermediate energy of 1.55 kcal/mol. Using the *ab initio* energies and the Boltzmann's distribution, $N_j/N_i = \exp[-(\epsilon_j - \epsilon_i)/RT]$, to calculate the relative equilibrium populations of the different isomers, a ratio of *ca.* 9:1:0.1 is obtained for isomers A:B:C at room temperature. This ratio fully supports the interpretation of the ^{1}H-NMR spectra of **9a** in the sense that these spectra would mainly result from isomer A with small contributions of isomer B, and the signals corresponding to isomer C would not be observed. More accurate relative energies would be obtained taking into account the effect of the solvent and by optimizing the geometries of isomers A−C at the *ab initio* 6-31G* level. The optimization is, however, limited by the size and low or nonexistent symmetry of the molecules. The use of a smaller basis set such us the 3-21G* is not recommended because it underestimates the folding of the DCNQI moiety as discussed above for **16**.

For compound **10a**, only the isomers with the benzooxathiin moiety pointing down (β < 180°) are found as energy minima, and their relative energies are given in Table 4. Due to the lack of symmetry, two *anti* isomers denoted as B and B′ are possible for **10a**. B corresponds to the isomer with the NCN group adjacent to the oxygen atom pointing to the oxygen, while for B′ the NCN group adjacent to the sulfur atom is that pointing to the heteroatom. At the PM3 level, the *anti* isomer B is calculated as the most stable and the maximum energy difference between the four isomers is smaller than 0.6 kcal/mol. At the 6-31G*//PM3 level, B continues to be the preferred structure, but now the energy differences increase to *ca.* 2 kcal/mol with the *syn* isomers A and C, and to 4.17 kcal/mol with the *anti* isomer B′. *Ab initio* calculations therefore show that the interactions between the cyano groups and the adjacent atoms in *peri* positions increase along the series O < CH < S, and that the most populated isomer for compounds **10** will be the *anti* structure B. These results support the assignment of the ^{1}H-NMR spectra performed above for **10a**.

Neutral Compounds: Electronic Structure. The electronic structure of compounds **9a** and **10a** was calculated using the PM3-optimized geometries and the VEH method. Compared to standard *ab initio* Hartree−Fock calculations, the VEH method yields one-electron molecular orbital energies of double-ζ quality and has the advantage of providing good estimates for the lowest-

(20) Ortí, E.; Viruela, R.; Viruela, P. M. *J. Mater. Chem.* **1995**, *5*, 1697.

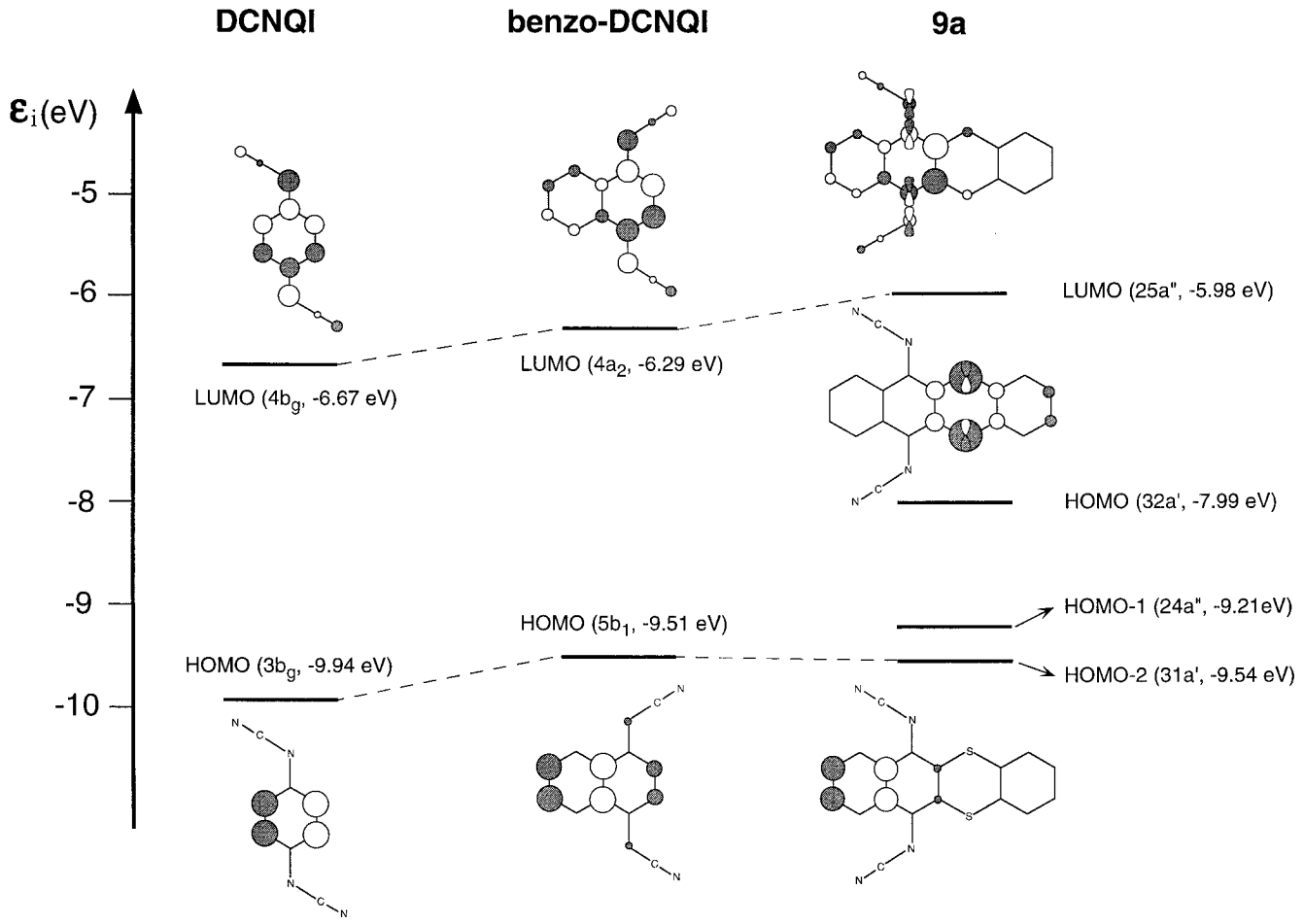

Figure 6. Molecular orbital diagram showing the VEH energies, symmetries, and atomic orbital (AO) composition of the HOMO and LUMO of DCNQI (C_{2h} symmetry), benzo-DCNQI (C_{2v} symmetry), and **9a** (C_s symmetry). Contributions from AOs other than π-type orbitals are due to the nonplanarity of the molecule.

energy optical transitions.[11,21] As previously discussed,[22] this feature is due to the fact that the VEH parameterization is not contaminated by any information coming from the unoccupied Hartree−Fock molecular orbitals (MOs) which are always calculated too high in energy. As a consequence, the energies of the virtual MOs afforded by the VEH method are expected to be of the same quality as for the occupied MOs.

Figure 6 sketches the energy, symmetry, and atomic orbital (AO) composition of the highest occupied molecular orbitals (HOMOs) and the lowest unoccupied molecular orbital (LUMO) calculated for **9a**. These orbitals are correlated with those of the parent DCNQI and those of benzo-DCNQI. The LUMO of **9a** spreads over the acceptor moiety and has the same AO composition than the LUMO of DCNQI and benzo-DCNQI. It has an energy of −5.98 eV and is destabilized with respect to DCNQI (−6.67 eV) by 0.69 eV. This destabilization already appears for benzo-DCNQI (−6.29 eV) and is due to the lateral extension of the π-system that reduces the bonding interactions in the DCNQI ring and introduces new antibonding interactions. The additional destabilization of 0.31 eV in passing from benzo-DCNQI to **9a** is due to the loss of planarity of the DCNQI moiety in **9a**. The destabilization calculated for the LUMO justifies the lower reduction potentials measured for benzo-DCNQI and **9a** compared to DCNQI. Hünig et al.[14] report a lowering of 0.20 V for the first reduction potential in passing from DCNQI (+0.39 V) to benzo-DCNQI (+0.19 V) potentials vs AgCl/Ag electrode. A similar lowering is measured here in passing fron DCNQI (+0.21 V) to **9a** (+0.05 V), potentials vs SCE. The LUMO of **10a** shows the same AO patterns as the LUMO of **9a** and appears at a similar energy of −6.08 eV in good accord with the almost identical reduction potentials measured for **9a** and **10a**.

As shown in Figure 6, the HOMO of **9a** is localized on the benzodithiin moiety and has no relation with the HOMO of DCNQI. It is calculated at −7.99 eV, i.e., *ca.* 2 eV above the HOMO of DCNQI (−9.94 eV). The latter actually correlates with the HOMO-2 of **9a** which is calculated at −9.54 eV and has the same AO composition than the HOMO of benzo-DCNQI. Identical trends are found for **10a** for which the HOMO lies at −8.02 eV.

The topologies of the HOMO and the LUMO of **9a** and **10a** suggest that the HOMO → LUMO electronic transition corresponds to an electron transfer from the benzodithiin or benzooxathiin moieties, acting as donors, to the acceptor benzo-DCNQI unit. This electronic transition would therefore appear at lower energies than in DCNQI. It is calculated at 2.01 eV (617 nm) for **9a** and at 1.94 eV (639 nm) for **10a** in quite good agreement with the lowest-energy absorption band observed experimen-

(21) (a) Viruela-Martín, R.; Viruela-Martín, P. M.; Ortí, E. *J. Chem. Phys.* **1992**, *97*, 8470. (b) Martín, N.; Segura, J. L.; Seoane, C.; de la Cruz, P.; Langa, F.; Ortí, E.; Viruela, P. M.; Viruela, R. *J. Org. Chem.* **1995**, *60*, 4077.

(22) Brédas, J. L.; Thémans, B.; André, J. M. *J. Chem. Phys.* **1983**, *70*, 6137.

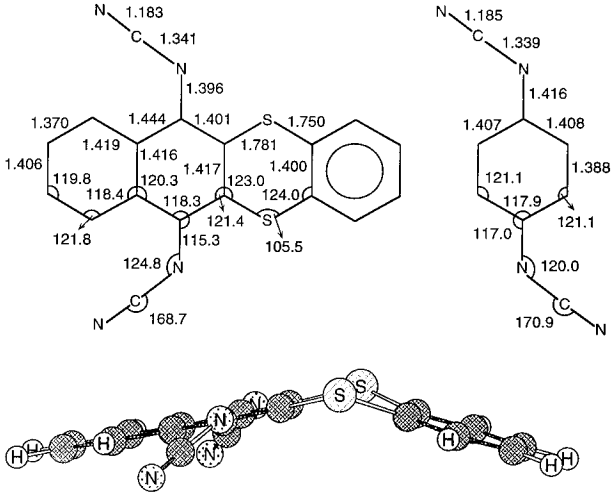

Figure 7. PM3-optimized geometries calculated for the dianions of **9a** (left) and DCNQI (right). Bonds are in angstroms and angles in degrees.

tally for **9a** (628 nm) and **10a** (669 nm). Theoretical calculations thus support the intramolecular charge-transfer nature of this band. For the analogous TCNQ derivatives **5** (515 nm) and **6** (594 nm), the charge-transfer band is observed at higher energies due to the larger folding of the TCNQ moiety that destabilizes the LUMO in a higher degree.[11] The HOMO → LUMO electronic transition is calculated to have an energy of 3.22 eV (385 nm) for benzo-DCNQI in good accord with the first absorption band recorded experimentally at 399 nm.[5a] The equivalent transition in **9a** (HOMO-2 → LUMO) experiences a hypsochromic shift due to the destabilization of the LUMO and appears at 3.56 eV (348 nm) in accord with the experimental value of 354 nm.

Reduced/Oxidized Compounds. To provide a deeper insight into the electrochemical behavior of compounds **9** and **10**, the molecular structure of the anions, dianions, and cations of **9a** and **10a** was optimized using the PM3 method. The reduction process mainly affects the DCNQI moiety because the LUMO, i.e., the orbital where the extra electrons are placed, is located on this moiety. This is illustrated in Figure 7, where the PM3-optimized geometry obtained for the dianion of **9a** is displayed together with that of $DCNQI^{2-}$. Reduction causes the aromatization of the DCNQI unit, the largest changes being found for the double bonds connecting the =N−CN units to the central backbone. They lengthen by *ca.* 0.1 Å in passing from the neutral molecule to the dianion: 1.300 Å (**9a**), 1.344 Å ($\mathbf{9a}^{\bullet-}$), 1.396 Å ($\mathbf{9a}^{2-}$). This lengthening reduces the steric interactions of the cyano groups making feasible the planarization of the DCNQI moiety.

The PM3 method predicts that the DCNQI moiety in the different isomers of the anions of **9a** and **10a** has a butterfly structure significantly less folded ($\alpha = 155-166°$, $\gamma = 23-32°$) than for the neutral molecules. This is, however, an artifact of the PM3 method since, as discussed above, it overestimates the folding of the DCNQI moiety. We have optimized the geometry of the anion of **16** at the *ab initio* 6-31G* level, and the molecule is obtained to be fully planar in contrast with the butterfly structure ($\alpha = 159.3°$, $\gamma = 29.8°$) afforded by the PM3 method. This result suggests that the DCNQI moiety in the anions of compounds **9** and **10** should be also planar.

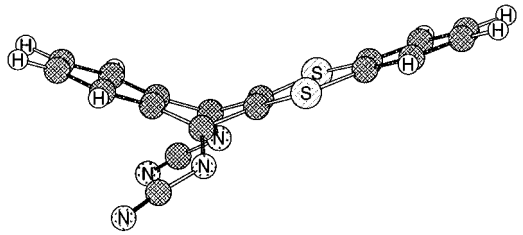

Figure 8. View showing the PM3 minimum-energy conformation adopted by the cation of **9a**.

The introduction of the second electron to form the dianion completes the aromatization of the DCNQI ring which now forms an aromatic naphthalene unit with the adjacent benzene ring (see Figure 7). The interactions of the cyano groups with the hydrogens in *peri* are alleviated by decreasing the C−C=N and N−C≡N angles from 118.7° and 172.9° in the neutral molecule to 115.3° and 168.7° in the dianion, respectively. The NCN groups are in addition twisted by *ca.* 34° around the N=C bonds, which have a marked single-bond character for the dianion.

The molecular structures obtained for the anions and dianions of the DCNQI derivatives **9a**, **10a**, and **16**, together with those previously reported for the TCNQ derivatives **5**, **6**, and TCAQ,[11] explain the different electrochemical behavior these compounds show upon reduction. For the DCNQI derivatives, the acceptor moiety in both the anions and dianions is planar and achieves a degree of aromaticity similar to that of $DCNQI^{\bullet-}$ and $DCNQI^{2-}$, respectively. The cyclic voltammograms of compounds **9**, **10**, and **16**[14] therefore present two-well separated one-electron reduction waves that, respectively, correspond to the formation of the radical anion and dianion. For the anions of TCNQ derivatives, the acceptor moiety is by contrast highly distorted from planarity.[11] The lack of planarity leads to less aromatic, i.e., less stable, anions, and as a consequence, the first reduction potential shifts to more negative values and collapses under a two-electron reduction wave with the second reduction potential.[11,14]

The low oxidation potentials measured for compounds **9** and **10** are due to the high-energy HOMO furnished by the donor benzodithiin and benzooxathiin units, respectively. The PM3 minimum-energy conformation calculated for the radical cation $\mathbf{9a}^{\bullet+}$ is given in Figure 8. The oxidation process mainly affects the sulfur bridges because the HOMO, from which the electron is extracted, is mostly located on them (see Figure 6). A quantity of 0.74 e is in fact computed to be extracted from the sulfur atoms in $\mathbf{9a}^{\bullet+}$. As a consequence, the benzodithiin moiety becomes planar and the S−C bonds shorten to 1.70 and 1.73 Å.

EPR Study. Intense EPR signals of the radical anions $\mathbf{9a}^{\bullet-}$ ($g = 2.0032 \pm 0.0001$) and $\mathbf{9b}^{\bullet-}$ ($g = 2.0032 \pm 0.0001$) were obtained upon reduction of **9a** and **9b** with potassium in 1,2-dimethoxyethane (DME). Care had to be taken not to push the reaction too far, in order to minimize formation of the corresponding dianions which are EPR silent. In the absence of air and humidity, $\mathbf{9a}^{\bullet-}$ and $\mathbf{9b}^{\bullet-}$ were very persistent in spite of their lower thermodynamic stability compared to the anion of the parent DCNQI (see log *K* values in Table 2). The EPR spectra of $\mathbf{9a}^{\bullet-}$ and $\mathbf{9b}^{\bullet-}$ are exemplified in Figure 9 by that of $\mathbf{9a}^{\bullet-}$. The hyperfine coupling constants (hfcc) of the ^1H and ^{14}N nuclei and line widths were derived from

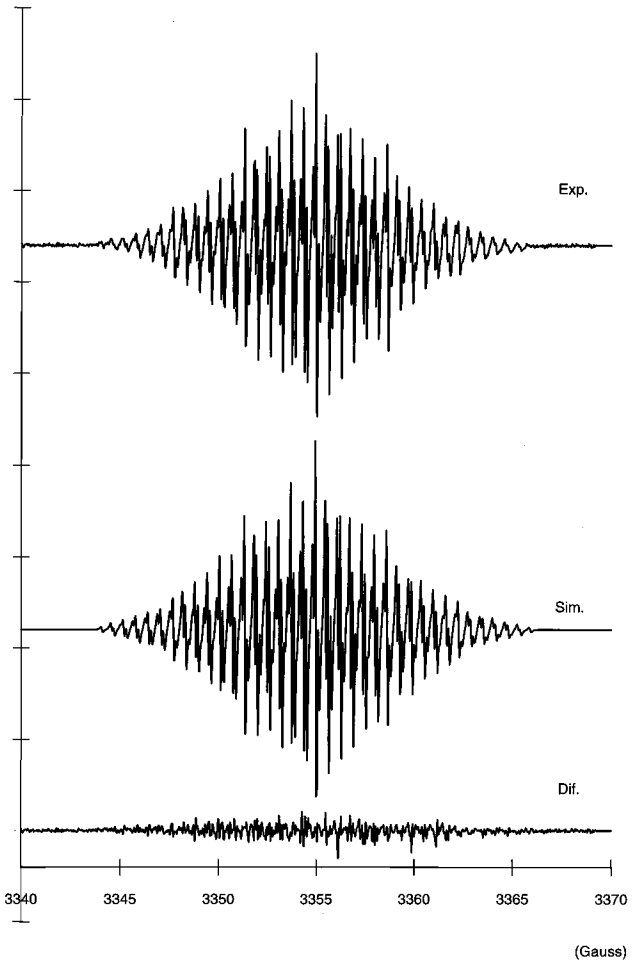

Figure 9. Experimental at 293 K, simulated, and difference EPR spectra of **9a**•−. The computer simulations made use of Lorentzian line shapes and the coupling constants and line widths given in Table 5.

computer simulations using a least-squares fitting procedure based on a Monte Carlo method that allows to take into account line width variations for each line of the spectrum.[23] An example of such simulated spectra is shown in Figure 9. The resulting coupling constants for **9a**•− and **9b**•− at 293 K are compiled in Table 5 along with the parameters defining the line widths and the spin densities calculated from the hfcc's using the McConnell's equation.[24] For both compounds, neither the hfcc's of ^{1}H and ^{14}N nuclei nor the line widths show a marked dependence on the temperature (220−300 K).

In spite of their large size and in contrast with that previously reported for the radical anions of *N*,*N*′-dicyano-*p*-quinonediimines such as DCNQI, benzo-DCNQI, and **16**,[25] the radical anions **9a**•− and **9b**•− exhibit extremely narrow line widths of *ca.* 0.007 mT. Thus, EPR simulations of both radical anions evidence that a slight line broadening takes place on going from low to high field and more markedly on passing from the center to the peripheries of the spectra. It is known that such kind of selective line broadenings are produced by the slow molecular tumbling rates of large radicals in solutions of moderate viscosity where the *g*-factor and hyperfine anisotropies are not completely averaged to zero. In such cases, the line widths, Γ, of lines produced by a set of equivalent nuclei with a M_I nuclear spin quantum number can be approximated by the following relationship[26]

$$\Gamma = A + BM_I + CM^2_I$$

where *A*, *B*, and *C* are the parameters given in Table 5 obtained from the simulated spectra. For radical anions **9a**•− and **9b**•−, the broadening of the EPR lines is more pronounced in the high-field half than in the low-field half of the spectra indicating that the B parameters associated with the lines produced by one type of ^{14}N nuclei are negative for both radical anions and, consequently, the coupling constants with such ^{14}N nuclei are positive.[26]

The hyperfine data obtained from the simulated spectra indicate the coupling with two pairs of equivalent protons, in addition to the coupling with the two pairs of nitrogen atoms (C═N and CN). The assignment of the coupling constants to nitrogens and protons in definite positions can be performed with the help of theoretical calculations. A general pattern of the spin distribution in the radical anion is provided by the LUMO which is displayed in Figure 6 for **9a**. The higher coupling constant (0.3642 mT) is attributed to the imine nitrogens (C═N) since they show the largest atomic orbital contributions to the LUMO. This assignment agrees with that performed by Gerson *et al.*[25] for other related radical anions. For **9a**•−, the ratio between the coupling constants of the imine and nitrile nitrogens is 2.88. This value is almost identical to that reported for **16** (2.70) and its 1,4-dimethoxy derivative (2.89).[25]

The ^{1}H couplings are ascribed to the four protons (H_a−H_d) of the benzo-DCNQI moiety since the contributions from the benzene rings of the benzodithiin moiety to the LUMO are very small. The fact that the EPR spectra indicate that hydrogens H_a−H_d are equivalent two by two suggests that the two NCN groups of **9a**•− and **9b**•− should mainly exist in only one *syn* configuration (C_s

Table 5. ^{1}H and ^{14}N Coupling Constants (mT), *A*, *B*, and *C* Line Width Parameters (mT), and Spin Densities for 9a•− and 9b•−

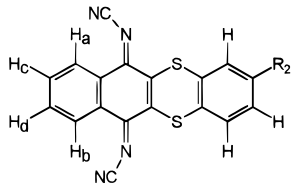

	hfcc[a]	*A*	*B*	*C*	spin dens (sd)[b]
9a•−	0.3642 (2N, C═N)	0.00693	−0.00023	0.00083	0.00663
	0.1263 (2N, CN)	0.00693			0.00230
	0.0615 (2H, H_a−H_b)	0.00693			0.00121
	0.0487 (2H, H_c−H_d)	0.00693			0.00096
9b•−	0.3560 (2N, C═N)	0.01088	−0.00193	0.00286	0.00648
	0.1259 (2N, CN)	0.01088			0.00229
	0.0608 (2H, H_a−H_b)	0.01088			0.00120
	0.0506 (2H, H_c−H_d)	0.01088			0.00100

[a] Experimental error ± 0.0001 mT. [b] For $^{14}N_s$:sd = hfcc/54.95; for ^1H_s: sd = hfcc/50.7.

(23) Kirste, B. *Anal. Chim. Acta* **1992**, *265*, 191.
(24) Weil, J. A.; Bolton, J. R.; Wertz, J. E. *Electron Paramagnetic Resonance. Elementary Theory and Practical Applications*; John Wiley: New York, 1994.
(25) Gerson, F.; Gescheidt, G.; Möckel, R.; Aumüller, A.; Erk, P.; Hünig, S. *Helv. Chim. Acta* **1988**, *71*, 1665.
(26) Hudson, A.; Luckhurst, G. R. *Chem. Rev.* **1969**, *69*, 191.

symmetry implies $H_a \equiv H_b$ and $H_c \equiv H_d$). This suggestion is supported by both ^{1}H-NMR data and theoretical calculations which, as discussed above, show that the *syn* isomer A (Figures 1 and 5) is the most stable configuration and would be the most abundant in solution. The *anti* isomer B, which would give rise to four different hydrogen coupling constants, is calculated to be significantly less stable, and its contribution to the ^{1}H NMR is hardly observed. The final assignment of the coupling constants of 0.0615 and 0.0487 mT to the H_a-H_b and H_c-H_d protons was performed on the basis of the spin populations calculated for isomer A of **9a**$^{\bullet-}$ at the PM3/UHF level. The spin population, calculated as the difference in the Mülliken populations for the α and β electrons, is larger for H_a and H_b (0.00097) than for H_c and H_d (0.00074). The ratio between these populations is 1.31 in very good agreement with the value of 1.26 deduced from the simulated spectra of **9a**$^{\bullet-}$. The coupling constants of the hydrogens attached to the benzodithiin moiety were not possible to be determined from the experimental data in agreement with the small values of the calculated spin populations (1 to 6 $\times$ 10^{-5}).

Summary and Conclusions

A new class of DCNQI derivatives (**9**, **10**) incorporating sulfur-containing donor moieties has been synthesized. The ^{1}H-NMR data recorded for these compounds evidence that they exist as a mixture of isomers resulting from the *syn*/*anti* isomerization of the NCN groups. The assignment of the signals of the *peri* hydrogens and the analysis of their evolution with temperature indicate that the preferred isomer corresponds to a *syn* configuration (A) for **9** and to an *anti* configuration (B) for **10**.

The UV-vis spectra of compounds **9** and **10** show a broad absorption in the visible that is assigned to an intramolecular charge-transfer. The electron donor/acceptor character of **9** and **10** has been further evidenced by cyclic voltammetry measurements. They give rise to stable radical cations upon oxidation and show two reversible one-electron reduction waves to the radical anion and dianion similarly to DCNQI.

The X-ray structural analysis performed for crystals of **9b** shows that molecules adopt a nonplanar conformation and are packed in vertical stacks where donor and acceptor moieties alternate their position. In agreement with this aggregation in mixed stacks [$\cdots$ (A$-$D)(D$-$A)-(A$-$D)$\cdots$], the electrical conductivity measured for **9b** is lower than 10^{-6} S cm^{-1}.

The molecular structure of compounds **9** and **10** has been investigated by performing theoretical calculations at both the semiempirical PM3 and *ab initio* 6-31G* levels. In accord with X-ray evidences, PM3 calculations predict that **9** and **10** have a nonplanar structure in which both the acceptor and the donor fragments are bent. 6-31G* calculations on the benzoannulated DCNQI **16** confirm that the butterfly-type structure adopted by the DCNQI moiety is more stable than the planar structure. The energy difference between these two structures is of only 2.75 kcal/mol. This small energy represents only one-tenth of that calculated for TCNQs and thus justifies the planar and butterfly structures observed for the DCNQI moiety in the crystal. The relative stabilities of the *syn*/*anti* configurations calculated at the 6-31G*//PM3 level show that the most stable structure corresponds to the *syn* isomer A for **9a** and to the *anti* isomer B for **10**, thus supporting the interpretation of the experimental ^{1}H-NMR spectra.

The most important difference when comparing the electronic structures of **9** and **10** with that of the parent DCNQI is the high-energy HOMO of the donor benzodithiin **9** and benzooxathiin **10** moieties. This level accounts for the low oxidation potentials measured for **9** and **10** and determines the appearance of the photoinduced intramolecular electron transfer observed in the visible due to the low-energy HOMO (located on the donor) $\rightarrow$ LUMO (spread on the acceptor) electronic transition.

The stability of the reduced/oxidized compounds has been studied by calculating the evolution of the molecular structure on the charging process. Reduction and oxidation, respectively, induce the planarization of the acceptor and donor moieties. In contrast to that reported for TCNQ derivatives,[11] the acceptor DCNQI moiety is already planar for **9**$^{\bullet-}$ and **10**$^{\bullet-}$, justifying the fact that stable radical anions are obtained for **9** and **10**. The intense EPR signals recorded for compounds **9** subject to reduction with potassium corroborate the formation of stable radical anions. The extremely narrow line widths (0.007 mT) allow for very fine simulations of the EPR spectra from which two values of ^{14}N and ^{1}H coupling constants are inferred. The coupling constants are assigned on the basis of theoretical calculations on **9a** and **9a**$^{\bullet-}$ and are consistent with the presence of the *syn* isomer A as the most abundant.

Experimental Section

Computational Method. The equilibrium geometries of compounds **9a**, **10a**, and **16** on both neutral and oxidized/reduced states were optimized using the PM3 semiempirical method[27] as implemented in the MOPAC-6.0 system of programs.[28] The PM3 method is a reparameterization of the MNDO approach[29] in which the AM1 form of the core$-$core interactions is used.[30] Compared to MNDO, the PM3 technique provides a much improved description of the interactions taking place between nonbonded atoms, e.g., hydrogen bonding or steric interactions.[27] The latter are specially important for the set of molecules studied in this work since they determine the planarity or nonplanarity of the system. The geometries of the parent DCNQI and its benzoannulated derivative **16** was further optimized at the *ab initio* level using the split valence 3-21G[31] and 6-31G*[32] basis sets. The latter includes polarization *d* functions on carbon and nitrogen atoms. Single point 6-31G* calculations were performed for the different isomers of **9a** and **10a** using the PM3-optimized structures. The *ab initio* calculations were done on IBM RS/6000 work stations using the GAUSSIAN 92 program.[33]

The geometries of neutral molecules and dianions were optimized within the restricted Hartree$-$Fock (RHF) formalism, while the spin-unrestricted Hartree$-$Fock (UHF)[34] approximation where electrons with different spins occupy different sets of orbitals was used for single-charged anions

(27) Stewart, J. J. P. *J. Comput. Chem.* **1989**, *10*, 209; **1989**, *10*, 221.
(28) Stewart, J. J. P. MOPAC: A General Molecular Orbital Package (version 6.0) *QCPE*, **1990**, *10*, 455.
(29) Dewar, M. J. S.; Thiel, W. *J. Am. Chem. Soc.* **1977**, *99*, 4899.
(30) Dewar, M. J. S.; Zoebisch, E. G.; Healy, E. F.; Stewart, J. J. P. *J. Am. Chem. Soc.* **1985**, *107*, 3902.
(31) (a) Binkley, J. S.; Pople, J. A.; Hehre, W. J. *J. Am. Chem. Soc.* **1980**, *102*, 939. (b) Gordon, M. S.; Binkley, J. S.; Pople, J. A.; Pietro, W. J.; Hehre, W. J. *J. Am. Chem. Soc.* **1982**, *104*, 2797.
(32) Hariharan, P. C.; Pople, J. A. *Chem. Phys. Lett.* **1972**, *16*, 217.
(33) Frisch, M. J.; Trucks, G. W.; Head-Gordon, M.; Gill, P. M. W.; Wong, M. W.; Foresman, J. B.; Johnson, B. G.; Schlegel, H. B.; Robb. M. A.; Replogle, E. S.; Gomperts, R.; Anches, J. L.; Raghavachari, K.; Binkley, J. S.; Gonzalez, C.; Martin, R. L.; Fox, D. J; DeFrees, D. J.; Baker, J.; Stewart, J. J. P.; Pople, J. A. Gaussian 92; Gaussian: Pittsburgh, PA, 1992.
(34) Pople, J. A.; Nesbet, R. K. *J. Chem. Phys.* **1954**, *22*, 571.

and cations. In all the PM3 calculations, the gradient norm achieved was lower than 0.05. The Berny analytical gradient method[35] was used for the *ab initio* optimizations, and the threshold values for the maximum force and the maximum displacement were 0.00045 and 0.0018 atomic units, respectively.

The electronic structure was investigated using the nonempirical valence effective Hamiltonian (VEH) pseudopotential technique.[36] This technique takes only into account the valence electrons and is based on the use of an effective Fock Hamiltonian where all the parameters used to build up the atomic potentials are optimized to reproduce the results of *ab initio* Hartree−Fock calculations. The VEH method is thus completely nonempirical since no experimental data enter the effective Fock Hamiltonian. It yields one-electron energies of *ab initio* double-ζ quality without performing any self-consistent-field (SCF) process or calculating any bielectronic integral. All the VEH calculations were performed using the atomic potentials previously optimized for hydrogen, carbon, and nitrogen atoms.[37]

Synthesis of Quinones 7 and 8. Benzo[*b*]naphtho[2,3-*e*]-[1,4]dithiin-6,11-quinone (**7a**), 2-methylbenzo[*b*]naphtho[2,3-*e*][1,4]dithiin-6,11-quinone (**7b**), benzo[*b*]naphtho[2,3-*e*][1,4]-oxathiin-6,11-quinone (**8a**), 2-methyl-benzo[*b*]naphtho[2,3-*e*][1,4]oxathiin-6,11-quinone (**8b**), 3-methylbenzo[*b*]naphtho[2,3-*e*][1,4]-oxathiin-6,11-quinone (**8c**), and 1,3-dimethylbenzo[*b*]-naphtho[2,3-*e*][1,4]oxathiin-6,11-quinone (**8d**) were prepared by following the method previously reported in the literature.[11]

Condensation of Quinones 7 and 8 with bis(trimethylsilyl)carbodiimide (BTC). General Procedure. To a solution of the corresponding quinone (1 mmol) in dry CH_2Cl_2 (25 mL), titanium tetrachloride (0.4 mL, 4.2 mmol) and bis-(trimethylsilyl)carbodiimide (BTC) (0.94 mL, 3.5 mmol) were added dropwise under argon atmosphere. The reaction mixture was stirred for 48 h (monitored by TLC), and then CH_2-Cl_2 (100 mL) was added. The solution obtained was poured on ice−water (100 g), and the mixture was vigorously stirred until reaching room temperature. The organic phase was separated and washed with plenty of water. After drying over magnesium sulfate, the solution was concentrated to *ca.* 10 mL, and the same volume of hexane was added. The precipitate formed was collected by filtration and recrystallized from the appropriate solvent.

Monocondensated compounds **11** and **12** can also be obtained as the major product by following the above general procedure, but using a quinone:BTC ratio of 1:2 and a shorter reaction time (2 h). Compound **11a** and the mixture of constitutional isomers **11b**, **12a**, and **12b** were thus obtained.

***N,N′*-Dicyanobenzo[*b*]naphtho[2,3-*e*][1,4]dithiin-6,11-quinonediimine (9a)**: yield 87%; mp > 300 °C (from acetonitrile); ^{1}H-NMR (300 MHz, $CDCl_3$) δ 8.94 (broad s, 2H), 7.87−7.84 (m, 2H), 7.42 (m, 2H), 7.35−7.34 (m, 2H); IR (KBr) 2180, 1560, 1525, 1460, 1300, 1270, 1170, 760 cm^{-1}; UV-vis ($CHCl_3$) λ_{max} (log ϵ) 628 (3.94), 354 (3.97), 247 (4.28); MS *m*/*e* 346 (M^+ + 2, 16), 344 (M^+,100), 318 (39), 303 (14), 292 (9), 154 (16), 146 (16), 120 (16), 102 (18), 82 (18), 76 (18), 69 (33). Anal. Calcd for $C_{18}H_8N_4S_2$: C, 62.79; H, 2.32; N, 16.26. Found: C, 62.73; H, 2.30; N, 16.18.

***N,N′*-Dicyano-2-methylbenzo[*b*]naphtho[2,3-*e*][1,4]dithiin-6,11-quinonediimine (9b)**: yield 92%; mp > 300 °C (from acetonitrile); ^{1}H-NMR (300 MHz, $CDCl_3$) δ 9.00 (broad s, 2H), 7.84−7.79 (m, 2H), 7.14−7.09 (m, 3H), 2.32 (s, 3H); IR (KBr) 2180, 1580, 1550, 1520, 1460, 1330, 1290, 760 cm^{-1}; UV-vis ($CHCl_3$) λ_{max} (log ϵ) 644 (3.74), 354 (3.97), 247 (4.28); MS *m*/*e* 360 (M^+ + 2, 12), 358 (M^+,100), 332 (23), 317 (12), 306 (13), 130 (14), 121 (19), 102 (23), 76 (15), 69 (22). Anal. Calcd for $C_{19}H_{10}N_4S_2$: C, 63.68; H, 2.79; N, 15.62. Found: C, 63.64; H, 2.79; N, 15.60.

X-ray Crystallographic Measurements. Crystal Data for Compound 9b: $C_{19}H_{10}N_4S_2$, MW = 358.435, orthorombic, *Pna* 2_1, a = 13.078 (1) Å, b = 15.767(3) Å, c = 7.776(1) Å, V = 1603.4(4) Å^3, z = 4, D_c = 1.48 g/mL, $F(000)$ = 736, μ = 30.24 cm^{-1}. Refined cell parameters were obtained from setting angles of 27 reflections. Hair shape black crystal (0.12 × 0.12 × 0.07 mm) was used for the analysis.

Data Collection. Automatic four circle diffractometer Philips PW 1100 with graphite orientated monochromated Cu Kα radiation. The intensity data were collected using the $\omega/2\theta$ scan mode between $2 < \theta < 65°$; two standard reflections were measured every 90 min with no intensity variation. A total of 1452 reflections were measured, and 547 were considered as observed ($I > 2\sigma(I)$ criterium). The data were corrected for Lorentz polarization effects.

Structure Solution and Refinement. The structure was solved by direct methods using SIR88[38] and DIRDIF92.[39] The poor quality of the crystals do not allow consideration of thermal parameters as anisotropic contributors. H atoms were calculated and included in a refinement as fixed contributors. A convenient weighting scheme was applied to obtain flat dependence in $\langle w\Delta^2F\rangle$ vs $\langle F_0\rangle$ and $\langle \sin\theta/\lambda\rangle$.[40] Final R (Rw) value was 15.9 (15.4) due to the bad quality of the crystal. According to the space group polarity z coordinate of S1 was fixed. Atomic scattering factors for the compound were taken from *International Tables for X-Ray Crystallography*,[41] and calculations were performed using XRAY80,[42] XTAL,[43] DIFABS,[44] HSEARCH,[45] and PARST.[46]

***N,N′*-Dicyanobenzo[*b*]naphtho[2,3-*e*][1,4]oxathiin-6,11-quinonediimine (10a)**: yield 83%; mp > 300 °C (from acetonitrile); ^{1}H-NMR (300 MHz, $CDCl_3$) δ 9.15 (broad s, 1H), 8.39−8.37 (d, 1H), 7.88−7.78 (m, 2H), 7.35−7.03 (m, 4H); IR (KBr) 2170, 1600, 1580, 1540, 1470, 1440, 1340, 1260, 1230, 770, 750 cm^{-1}; UV-vis ($CHCl_3$) λ_{max} (log ϵ) 669 (3.05), 348 (4.29), 276 (4.00), 240 (4.14); MS *m*/*e* 330 (M^+ + 2, 6), 328 (M^+, 100), 303 (13), 262 (6), 146 (9), 120 (16), 76 (12), 69 (11). Anal. Calcd for $C_{18}H_8N_4OS$: C, 65.85; H, 2.44; N, 17.07. Found: C, 65.84; H, 2.34; N, 16.92.

***N,N′*-Dicyano-2-methylbenzo[*b*]naphtho[2,3-e][1,4]oxathiin-6,11-quinonediimine (10b)**: yield 93%; mp > 300 °C (from acetonitrile); ^{1}H-NMR (300 MHz, $CDCl_3$) δ 9.13 (broad s, 1H), 8.38−8.36 (d, 1H), 7.84−7.77 (m, 2H), 7.21−7.20 (d, 1H), 7.15 (s, 1H), 6.91−6.88 (m, 1H), 2.30 (s, 3H); IR (KBr) 2185, 1600, 1550, 1490, 1350, 1270, 1240, 1170, 820, 670 cm^{-1}; UV-vis ($CHCl_3$) λ_{max} (log ϵ) 692 (3.06), 354 (4.35), 304 (4.11), 276 (4.04), 240 (3.24); MS *m*/*e* 344 (M^+ + 2, 10), 342 (M^+, 100),

(35) Schlegel, H. B. *J. Comput. Chem.* **1982**, *3*, 214.
(36) (a) Nicolas, G.; Durand, Ph. *J. Chem. Phys.* **1979**, *70*, 2020; **1980**, *72*, 453. (b) André, J. M.; Burke, L. A.; Delhalle, J.; Nicolas, G.; Durand, Ph. *Int. J. Quantum Chem. Symp.* **1979**, *13*, 283. (c) Brédas. J. L.; Chance, R. R.; Silbey, R.; Nicolas, G.; Durand, Ph. *J. Chem. Phys.* **1981**, *75*, 255.
(37) (a) André, J. M.; Brédas, J. L.; Delhalle, J.; Vanderveken, D. J.; Vercauteren, D. P.; Fripiat, J. G. In *Modern Techniques in Computational Chemistry: MOTECC-90*; Clementi, E., Ed.; Escom: Leiden, The Netherlands, 1990; p 745. (b) Brédas, J. L.; Thémans, B.; André, J. M. *J. Chem. Phys.* **1983**, *78*, 6137.
(38) Cascarano, G.; Giacovazzo, C. Dip. Geomineralogico-Univ. of Bari. Burla, M. G.; Polidori, G. Dip. Scienze de la Terra-Univ. of Perugia. Camalli, M.; Spagna, R. Ist. Strutt. Chimica CNR-Monterotondo Stazione, Roma. Viterbo, D. Dip. di Chimica, Univ. della Calabria, Consenza. SIR88, 1988.
(39) The DirDif Program System. Beurskens, P. T.; Admiral, G.; Behm, H.; Beurskens, G.; Bosman, W. P.; García-Granda, S.; Gould, R. O.; Smykalla, C. *Zeitsch. Krist.* **1990**, *4*, 99.
(40) Martínez-Ripoll, M.; Cano, F. H. PESOS. A computer program for the automatic treatment of weighting schemes. Instituto Rocasolano C.S.I.C. Serrano 119, 28006 Madrid, Spain.
(41) *International Tables for X-Ray Crystallography*; Birmingham Press: Birmingham, U.K., 1974; Vol. IV.
(42) Hall, S. R.; Stewart, J. M. XTAL System, University of Western Australia, Perth, Australia, 1990.
(43) Stewart, J. M.; Kundell, F. A.; Baldwin, J. C. The X-Ray76 Computer Science Center, University of Maryland, College Park, MD, 1976.
(44) Walker, N.; Stuart, D. DIFABS, An empirical method for correcting diffractometer data for absorption corrections. *Acta Crystallogr.* **1983**, *A39*, 158.
(45) Fayos, J.; Martinez-Ripoll, M. HSEARCH. A computer program for the geometric calculations of H atom Coordinates; Instituto Rocasolano, C. S. I. C., Madrid, Spain, 1978.
(46) Nardeli, M. PARST. *Comput. Chem.* **1983**, *7*, 95.
(47) The author has deposited atomic coordinates for this structure with the Cambridge Crystallographic Data Centre. The coordinates can be obtained, on request, from the Director, Cambridge Crystallographic Data Centre, 12 Union Road, Cambridge, CB2 1EZ, UK.

316 (5). Anal. Calcd for $C_{19}H_{10}N_4OS$: C, 66.66; H, 2.92; N, 16.37. Found: C, 66.59; H, 3.12; N, 16.31.

***N,N′*-Dicyano-3-methylbenzo[*b*]naphtho[2,3-*e*][1,4]oxathiin-6,11-quinonediimine (10c)**: yield 89%; mp > 300 °C (from acetonitrile); ^{1}H-NMR (300 MHz, $CDCl_3$) δ 9.14 (broad s, 1H), 8.38−8.36 (d, 1H), 7.87−7.77 (m, 2H), 7.21−7.18 (d, 1H), 6.98−6.95 (d, 1H), 6.84 (m, 1H), 2.28 (s, 3H); IR (KBr) 2180, 1605, 1575, 1550, 1480, 1355, 1345, 1260, 1240, 1200, 900 cm^{-1}; UV-vis ($CHCl_3$) λ_{max} (log ϵ) 688 (3.09), 352 (4.39), 310 (4.13), 276 (4.02), 268 (3.99), 241 (4.24); MS *m*/*e* 344 (M^+ + 2, 8), 342 (M^+, 100), 316 (3). Anal. Calcd for $C_{19}H_{10}N_4OS$: C, 66.66; H, 2.92; N, 16.37. Found: C, 66.62; H, 2.92; N, 16.31.

***N,N′*-Dicyano-1,3-dimethylbenzo[*b*]naphtho[2,3-*e*][1,4]oxathiin-6,11-quinonediimine (10d)**: yield 77%; mp > 300 °C (from acetonitrile); ^{1}H-NMR (300 MHz, $CDCl_3$) δ 9.07 (broad s, 1H), 8.36 (s, 1H), 7.85−7.76 (m, 2H), 6.80 (s, 1H), 6.62 (s, 1H), 2.44 (s, 3H), 2.21 (s, 3H); IR (KBr) 2180, 1610, 1600, 1560, 1540, 1470, 1350, 1340, 1270, 1220, 1200, 900 cm^{-1}; UV-vis ($CHCl_3$) λ_{max} (log ϵ) 717 (3.18), 352 (4.49), 306 (4.20), 276 (4.10), 267 (4.10), 242 (4.43). Anal. Calcd for $C_{20}H_{12}N_4OS$: C, 67.41; H, 3.37; N, 15.73. Found: C, 67.42; H, 3.45; N, 15.65.

6-(Cyanoimino)benzo[*b*]naphtho[2,3-*e*][1,4]dithiin-11-one (11a): yield 69%; mp > 300 °C (from acetonitrile); ^{1}H-NMR (300 MHz, $CDCl_3$) δ 9.00 (broad s, 1H), 8.17 (m, 1H), 7.75 (m, 2H), 7.4−7.0 (m, 4H); IR (KBr) 2170, 1650, 1590, 1570, 1530, 1480, 1300, 770, 700 cm^{-1}. Anal. Calcd for $C_{17}H_8N_2OS_2$: C, 63.73; H, 2.52; N, 8.74. Found: C, 63.68; H, 2.59; N, 8.65.

6-(Cyanoimino)-2-methylbenzo[*b*]naphtho[2,3-*e*][1,4]dithiin-11-one and 11-(Cyanoimino)-2-methylbenzo[*b*]naphtho[2,3-*e*][1,4]dithiin-6-one (11b): yield 57%; mp > 300 °C (from acetonitrile); ^{1}H-NMR (300 MHz, $CDCl_3$) δ 8.9 (broad s, 1H), 8.2 (m, 1H), 7.8 (m, 2H), 7.3−7.1 (m, 3H), 2.3 (s, 3H); IR (KBr) 2170, 1650, 1590, 1570, 1530, 1480, 1300, 760, 700 cm^{-1}. Anal. Calcd for $C_{18}H_{10}N_2OS_2$: C, 64.65; H, 3.02; N, 8.37. Found: C, 64.68; H, 2.99; N, 8.45.

6-(Cyanoimino)benzo[*b*]naphtho[2,3-*e*][1,4]oxathiin-11-one and 11-(Cyanoimino)benzo[*b*]naphtho[2,3-*e*][1,4]oxathiin-6-one (12a): yield 41%; mp > 300 °C (from acetonitrile); ^{1}H-NMR (300 MHz, $CDCl_3$) δ 9.1 (broad s, 1H), 8.3−8.1 (m, 1H), 7.7 (m, 2H), 7.2−6.8 (m, 4H); IR (KBr) 2170, 1650, 1600, 1550, 1480, 1300, 770, 700 cm^{-1}. Anal. Calcd for $C_{17}H_8N_2O_2S$: C, 67.10; H, 2.63; N, 9.22. Found: C, 67.08; H, 2.59; N, 9.15.

6-(Cyanoimino)-2-methylbenzo[*b*]naphtho[2,3-*e*][1,4]oxathiin-11-one and 11-(Cyanoimino)-2-methylbenzo[*b*]naphtho[2,3-*e*][1,4]oxathiin-6-one (12b): yield 33%; mp > 300 °C (from acetonitrile); ^{1}H-NMR (300 MHz, $CDCl_3$) δ 9.1 (broad s, 1H), 8.3 (m, 1H), 7.8 (m, 2H), 7.4−7.0 (m, 3H), 2.4 (s, 3H); IR (KBr) 2170, 1650, 1590, 1570, 1530, 1480, 1300, 770, 700 cm^{-1}. Anal. Calcd for $C_{18}H_{10}N_2O_2S$: C, 68.79; H, 3.18; N, 8.92. Found: C, 68.68; H, 2.99; N, 8.85.

Acknowledgment. This work has been supported by the DGICYT Projects PB92-0237, PB91-0935, MAT94-0797 and by the Generalitat Valenciana. The group from the University of Valencia is grateful to Prof. F. Tomás for fruitful discussions and to W. Díaz for technical assistance.

JO952274O